TR-2
1966

Texas Water Resources Institute
make every drop count

Flume Studies of Sediment Transportation in Shallow Flow with Simulated Rainfall

F.M. Nail

Texas Water Resources Institute

Texas A&M University

Flume Studies of Sediment Transportation in Shallow Flow with Simulated Rainfall

by

Frank Mitchell Nail

Water Resources Institute
Texas A&M University
January 1966

This investigation was supported in part by
Public Health Service Research Grant WP00757-02
From the Division of Water Supply and Pollution Control

ACKNOWLEDGMENTS

The author wishes to gratefully acknowledge the guidance and assistance given by Dr. E. T. Smerdon during the course of this study. Thanks are extended to Drs. O. R. Kunze, J. R. Runkles, and R. A. Clark for their review and comments.

Sincere appreciation is expressed to Professor W. B. Davis for his many helpful suggestions during this study. Thanks are also expressed to Professor J. G. Darroch who assisted in the statistical design which was used.

Acknowledgment is further extended to the Agricultural Engineering Department staff who provided facilities and assistance. The U. S. Public Health Service is sincerely thanked for the financial assistance which made this work possible.

TABLE OF CONTENTS

LIST OF FIGURES

LIST OF TABLES

CHAPTER I

INTRODUCTION

During the past decade, the pollution of the nation's waters has caused increased concern. Conservation of water as pertains both to supply and water quality has been accelerated to make the most efficient use of resources and thereby meet existing needs. Rapid population increases, with resulting industrial and urban expansion, have not only created greater demands on existing water resources, but have limited their usefulness by increasing pollution from factory wastes and sewage and adding more sediments by the resultant increases in erosion.

The problem of water pollution is not new. Throughout history, nature's hydrologic cycle has been disrupted by civilization. Land has been denuded by the removal of forests and by cultivation and urban construction. One result of man's activity was observed some 8,000 years ago, soon after the Sumerians initiated irrigation on the plains of Mesopotamia (18). Soon after the forests on the upland slopes of the Tigris and Euphrates Rivers were cut, the irrigation canals were filled with silt. The silt along the banks of the canals became so high that reconstruction of the canals was impossible; as a result, the Sumerian civilization began its decay. In the sixth century B. C., the Romans had a similar experience after constructing a storm sewer—the Cloaca Maxima—to dispose of sewage from Rome and to drain the Campagna swamp.

The Maya Indians of southern Mexico appear to have also suffered a decline as a result of water erosion. They obtained farmlands by burning forests; torrential tropical rains soon swept their unprotected topsoil away, crop yields decreased, and the Mayan culture crumpled.

Now, the United States is faced with the possibility of having similar problems. Silt is a major pollution problem resulting from the lack of water and soil conservation efforts. The control of soil movement should substantially reduce both erosion and water pollution.

Many conservation measures for checking the movement of soil have received extensive attention. Some of the more common are contour plowing and terracing, development of flood control projects, reforestation programs, and the planting of quick-growing grasses and legumes. Although these measures are effective,the extent of their usage has not been sufficient to control or eliminate problems of pollution by eroded sediments.

The effects of silt or sediment on water resources are considered detrimental to water supplies, recreation, commercial fishing, flood control, and power generation (16). Although extensive research has been directed toward reducing or eliminating silt at its source and at the point where it becomes a problem, few studies have been directed at its removal between its origin and its point of deposition.

The movement of sediment particles from the point of detachment to the place of their ultimate deposition may be a distance of inches or hundreds of miles. The sediment moves through streams which may begin as rivulets a fraction of an inch wide. As the sediment moves toward the point of deposition, the size of the stream will increase, but some of the distance will be in channels no more than a few feet wide and less than a foot deep.

A review of the literature reveals little about the transportation of sediment in these shallow streams and even less about the effects of rainfall on sediment transport in these streams. This is the portion of sediment transport to which this study is directed. The objectives of this study are:

1. To determine the effect of rainfall on total sediment transport in a shallow stream.
2. To establish a relationship between changes in flow conditions due to simulated rainfall and the resultant changes in sediment concentrations.
3. To determine how simulated rainfall affects suspended sediment transport capacity.
4. To apply the results of this study where they may be appropriate to natural streams.

Review of Literature

Sediment Transport

The sediment transport problem can be approached by two methods (8). One is to note and record the pertinent dimensions, discharges, and sediment loads in canals and rivers that are stable. Empirical formulas may then be developed correlating these data to the sediment transport capacity of a stream in a specific region. The other method is to determine the forces and other physical factors which cause sediment particles to be transported along the streambed or in suspension.

The first of these, the empirical procedure, has been used often for designing stable channels. Empirical formulas generally cannot encompass all the factors affecting sediment transportation. Furthermore, they must be taken from a natural environment to be of practical value. Hence, only those that are commonly used will be reviewed in this study.

The second method, the theoretical approach to sediment transport, has been studied for many years. According to Leliavsky (8), it was begun by Dupuit and Dubuat, who divided their studies of sediment transportation into two portions by defining "suspended load" and "bedload." Suspended load was defined as the smaller particles in a stream picked up from the bed of the channel or scoured from the sides and carried in the flow for an appreciable distance or time. Bedload was

defined as the larger particles of the transported material which were pushed or rolled along the bed of the channel, or those particles which jumped from the crest of one ripple on the streambed to another.

This distinction allowed the study of sediment transportation to be divided into two categories, suspension and traction (17). When a particle of sediment is in suspension, its velocity is assumed to be the same as that of the transporting media, whereas a particle being moved as bedload travels at lower velocities.

Bedload Transport

Leliavsky (8) reported that studies of bedload transport or transportation by tractive forces were begun by Brahams and Airy. They considered the drag or tractive force exerted on a particle by flowing water, which according to Newton, was equal to

$$\xi \gamma_s \pi r^2 V_{cr}^2 , \qquad (1)$$

where ξ is a shape factor (0.79 for spheres), γ_s is the specific weight of the particle, r is its radius, and V_{cr} is the critical bottom velocity. The friction force between the channel bed and the individual particle is

$$\phi(\gamma_s - \gamma) \frac{4}{3} \pi r^3, \qquad (2)$$

where ϕ is the coefficient of friction, $(\gamma_s - \gamma)$ is the difference between the specific weight of the particle and water, and $\frac{4}{3}\pi r^3$ is the volume

of the particle. The friction force was equated to the tractive force. Braham's equation resulted which related critical bottom velocity to particle size. This equation can be written as

$$V_{cr} = KW^{1/6}, \tag{3}$$

where K is a constant of proportionality, and W is the weight of the particle, proportional to the cube of its radius.

Due to the obvious limitations of such an equation which only considers the weight of a particle, an equation for tractive force was developed which considered other flow conditions, including the depth of flow and the slope of the energy gradient. All of the forces parallel to the main axis of the current were considered in the development of the basic equation for the tractive force. The tractive force, τ_o, can be expressed as

$$\tau_o = \gamma d S_e, \tag{4}$$

where d is the depth of flow, and S_e is the slope of the energy gradient. According to Leliavsky (8), this equation is believed to have been first proposed by P. duBoys in 1879. It was developed as follows (4) (see Figure 1).

For uniform flow, defined as that flow which is neither accelerating nor decelerating, a force parallel to the channel bed exists as a result of the channel slope. This force for a channel section of length, L, and cross-sectional area, A, and a channel slope angle, θ, can be

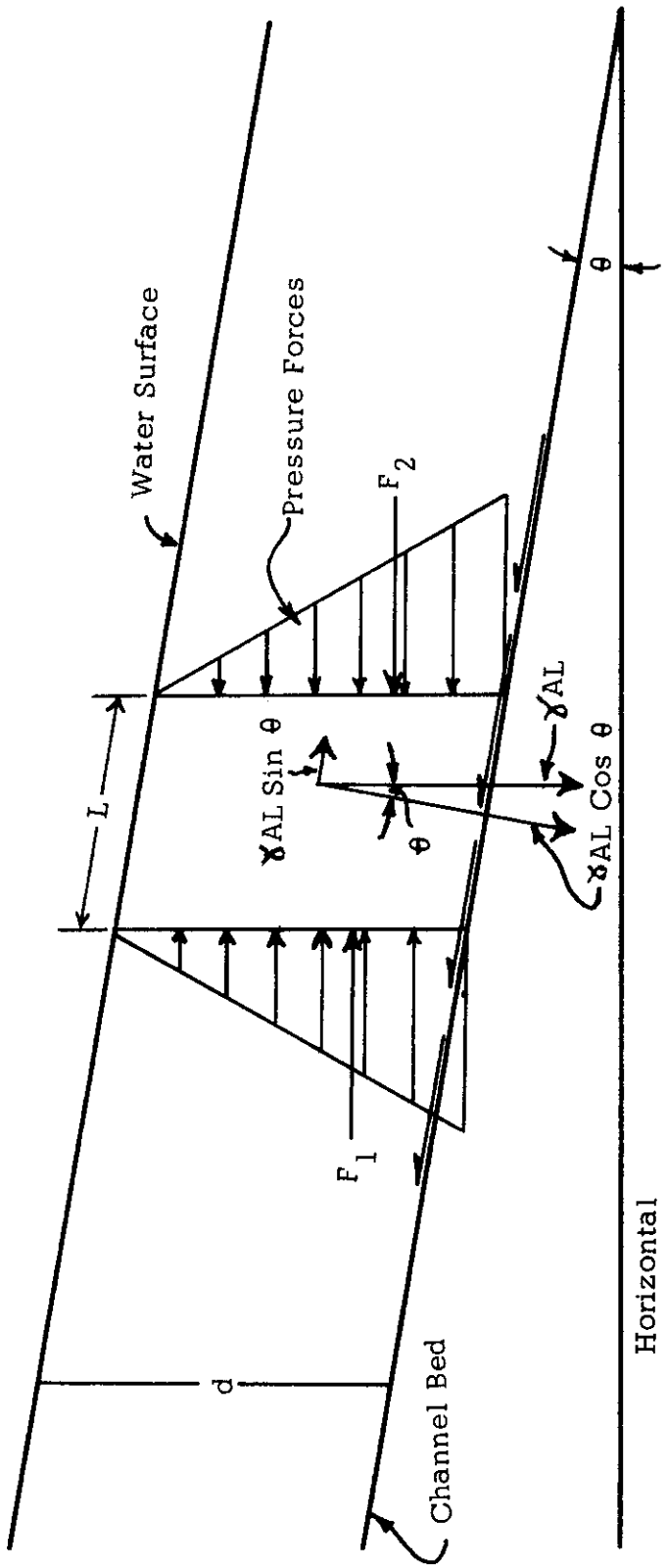

Figure 1. The Tractive Force Diagram.

expressed as

$$\gamma AL \text{ Sin } \theta. \tag{5}$$

This force, for the case of uniform flow, is balanced by bed friction. Thus, the forces parallel to the bed may be summed:

$$\Sigma F_H = F_1 + \gamma AL \text{ Sin } \theta = F_2 + \text{bed friction}. \tag{6}$$

Since F_1 and F_2, the pressure forces at each side of the channel section, L, are equal in uniform flow, they may be canceled. The friction at the air-water interface, the couple formed by F_1 and F_2, and the fact that $\gamma AL \text{ Sin } \theta$ is not quite parallel to F_1 and F_2 are insignificant for those slopes usually encountered in open channels. The total bed friction force acting on a section of channel with length, L, is the product of the tractive force (shear) and the wetted area, A, of the sector. That is

$$\gamma AL \text{ Sin } \theta = \tau_o PL, \tag{7}$$

where P is the wetted perimeter and for small θ, Sin θ = Tan θ = channel bed slope, S_o. For a wide channel, the hydraulic radius, R, is assumed to be equal to the average depth, so for two-dimensional flow,

$$\tau_o = \gamma d S_e. \tag{8}$$

Suspended Load Transport

When the transportation of sediment by suspension is evaluated, the properties of the sediment and the hydraulic characteristics of the flow must be considered (13). The properties of sediment which are important include size, shape, and specific gravity. Since natural noncohesive sediment must be evaluated in these terms by a frequency distribution of the soil properties, these properties must be expressed as parameters which are typical to the aggregate behavior of the sediment. Of these properties, size is the most important, as the others tend to vary accordingly in noncohesive natural sediments.

One of the first methods of considering both the suspended sediment and the flow properties of the fluid was Stokes' Law, which disregarded inertia and made the drag dependent on viscous resistance alone. Stokes' Law can be written

$$w = \frac{2(\gamma_s - \gamma)gr^2}{9\eta} \qquad (9)$$

where w is the fall velocity of the particle, g is the acceleration due to gravity, and η is the dynamic viscosity of the liquid (13). Stokes' Law is accepted for the vertical velocity of spheres at low values of the Reynolds number ($R_e = \frac{wD}{\nu} < 0.1$, where D is the diameter of the spheres and ν is the kinematic viscosity of the fluid). For higher Reynolds numbers at which the inertial effects cannot be ignored, the value of the fall velocity must be determined experimentally.

The downward flux of materials suspended in still water may be adequately described by Stokes' Law; however, this description is not complete for flowing water. In flowing water, suspended material will stay in suspension indefinitely. Therefore, there must be forces within the flow which produce an upward flux of the sediment proportional to the downward flux due to gravity.

Several theories have been proposed to describe this upward flux. Among the earliest of these were the Dupuit-Flamant theories which considered the forces acting on the individual grains (8). Some of these forces involved an interaction between the forces of the current and the opposing forces from other grains on the channel bed. Others considered differences in the magnitudes and directions of the velocities of adjacent sheets of the current. This explanation of suspended sediment transport is now rejected.

Currently, the only adequate explanation of suspended sediment transport is based on the turbulence theory. Turbulence is defined as the condition of a fluid after the eddies generated in the zone of instability spread through the fluid causing a disruption of the entire flow pattern. In turbulent flow, eddies of sizes and intensities that depend on many factors exist constantly.

Studies of turbulent flow reveal that the distribution of velocity varies with the cross section of a channel. In wide streams, the

vertical velocity distribution is logarithmic. Von Karman (Rouse, 12) has developed a velocity defect law from experiments which indicate that in turbulent flow, the intensity of shear and the eddy viscosity are directly proportional to the shear velocity, which is defined as $\sqrt{gdS_e}$ or $\sqrt{\tau_o/\rho}$, and is inversely proportional to the distance from the boundary. Von Karman's equation may be written as

$$\frac{V}{\bar{V}} = 1 + \left(\frac{\sqrt{gdS_e}}{k\bar{V}}\right) \left(1 + \ln \frac{y}{d}\right), \qquad (10)$$

where V is the velocity at any point, $\bar{V}$ is the mean velocity, y is the distance from the bottom at which V was measured, and k is von Karman's constant, which is generally assumed as 0.4, determined from experiments with clear water pipe flow.

Turbulent flow can be visualized as being divided into sheets of fluid having one velocity. These sheets are traversed by eddies, and in this manner the flow tends to establish a condition of equilibrium by a mixing process, or the penetration of each sheet with eddies of varying velocities. If ℓ is the average depth of these eddy penetrations and $\bar{u}$ is the average velocity at their original level, the mixing process must be proportional to $\ell\,\bar{u}$. It follows that the shear, τ, between adjacent sheets in the flow is related to the velocity gradient and the mixing intensity. This relationship can be expressed as

$$\tau = \rho\beta\ell\bar{u}\frac{dV}{dy} = \rho\epsilon_m\frac{dV}{dy}, \qquad (11)$$

where ρ is the mass density of the fluid, β is a constant, and $\frac{dV}{dy}$ is the velocity differential with respect to y. Therefore, ϵ_m is equal to $\beta \ell \bar{u}$ and is known as the "momentum transfer coefficient" or "kinematic eddy viscosity." The kinematic eddy viscosity is analogous to the kinematic viscosity in laminar flow. Because eddies vary randomly in time and size, the conclusion may be drawn that the turbulence theory is basically a statistical problem.

As mentioned, in turbulent flow water particles travel from one sheet of fluid to another. It follows that sediment grains will tend to travel from one sheet to another in the same manner as the water. Under equilibrium conditions, the rate at which sediment is carried upward by the mixing process must equal the rate at which the sediment settles. Thus, a formula can be developed for the transfer of suspended sediment in a manner similar to the equation for momentum transfer (Equation 11). As in its development, $\ell \bar{u}$ determines the intensity of the mixing process, making

$$G = -\beta \ell \bar{u} \frac{ds}{dy} \quad , \tag{12}$$

where G is the mass rate of transfer of suspended particles, and s is the sediment concentration. In this equation β, ℓ, and $\bar{u}$ are not necessarily the same as in the equation for shear.

Every size and weight of particle has a maximum fall velocity, w, for a given temperature. The downward flux of sediment at any point in the flow is the product of the sediment concentration, s, and the settling velocity, w. Therefore, for equilibrium, the downward flux of sediment must equal the upward flux giving

$$-\beta \ell \bar{u} \frac{ds}{dy} = sw \quad \text{or} \quad sw + \epsilon_s \frac{ds}{dy} = 0. \tag{13}$$

(ϵ_s, the sediment transfer coefficient, is not necessarily equal to the momentum transfer coefficient, ϵ_m.) Integrating Equation (13) gives

$$\ln \frac{s}{s_a} = -w \int_a^y \frac{dy}{\epsilon_s}, \tag{14}$$

where s_a is the sediment concentration at the arbitrary height, a, above the bed. This formula (Leliavsky, 8) is a result of the efforts of Hurst, Schmidt, O'Brien, and von Karman. It replaced the Dupuit-Flamant solution.

To integrate Equation (14), ϵ_s must be expressed as a function of y. Assuming ϵ_s to be constant from the distance a to y above the bed,

$$\frac{s}{s_a} = e^{-\frac{w}{\epsilon_s}(y-a)}. \tag{15}$$

The interrelation between ϵ_s and y is unknown. However, ϵ_s is often assumed to be equal to ϵ_m. Therefore,

$$\ln \frac{s}{s_a} = -\rho w \int_a^y \frac{dV/dy}{\tau} \, dy \quad . \tag{16}$$

The integral term contains dV/dy and τ which must be expressed in terms of y to be integrated. Using von Karman's universal velocity defect law, an equation can be developed to describe suspended sediment distribution as follows:

1. $k(V-V_{max})V_* = \ln y - \ln y_{max}$ (17)

   where V_* is the shear velocity. (This is an alternate method of writing Equation (10), von Karman's universal velocity defect law.)

2. The change in velocity with respect to y is

   $$\frac{dV}{dy} = \frac{V*}{ky} \quad . \tag{18}$$

3. y_{max} equals d for the maximum velocity of flow, and the shear is zero at that point.

4. Since the shear, τ, is zero at d, and a maximum at the bed,

   $$\tau = \tau_o \left(\frac{d-y}{d}\right) \quad ,$$

   where $\tau_o = \gamma d s_e$, substitution of Equations (18) and (19) into Equation (16) yields

   $$\ln \frac{s}{s_a} = \frac{w}{k\sqrt{\frac{\tau_o}{\rho}}} \int_a^y \frac{dy}{y\left(\frac{d-y}{d}\right)} \quad . \tag{20}$$

Upon integration,

$$\frac{s}{s_a} = \left(\frac{d-y}{y} \times \frac{a}{d-a}\right)^{\frac{w}{k\sqrt{\tau_o/\rho}}} , \qquad (21)$$

which is O'Brien's (11) equation for suspended sediment distribution.

Engineering Calculations for Sediment Transport

O'Brien's equation permits a direct determination of the concentration of sediment at any depth when the concentration at a reference depth is known. A method of using this equation may be obtained from the following development:

1. A value of ϵ_s may be estimated (assuming $\epsilon_s = \epsilon_m$) by considering a wide stream,

$$\epsilon_s = \frac{\tau_o (1-y/d)}{\rho \frac{dV}{dy}} = \frac{\sqrt{gdS_e}^{\,2} (1-y/d)}{\frac{dV}{dy}} . \qquad (22)$$

2. Differentiation of Equation (10) gives Equation (18).

3. Therefore,

$$\epsilon_s = ky \sqrt{gdS_e} \left(\frac{d-y}{d}\right) . \qquad (23)$$

Within this development, the following assumptions must be made:

$$\tau = \tau_o \left(1 - \frac{y}{d}\right) = \rho \epsilon_s \frac{dV}{dy} . \qquad (24)$$

Equation (23) indicates that ϵ_s is zero at the stream top and bottom and is a maximum at the middle (7). Again, however, a constant value is desirable for ϵ_s. So, from Equation (23) the average value of ϵ_s, used as the constant, can be calculated as follows:

$$\epsilon_{s\,avg.} = \frac{1}{d}\int_0^d \epsilon_s dy = \frac{1}{d}\int_0^d k\sqrt{gdS_e}\,(y - \frac{y^2}{d})\,dy$$

$$\epsilon_{s\,avg.} = 0.167\,k\,d\sqrt{gdS_e} = \frac{d\sqrt{gdS_e}}{15} . \qquad (25)$$

Substituting this value into Equation (15), the equation for sediment distribution becomes

$$\frac{s}{s_a} = e^{-15t(y-a)/d} , \qquad (26)$$

where $t = \frac{w}{\sqrt{\tau_o/\rho}}$. This relation plots as a straight line on semi-logarithmic paper. The concentration for any depth can be determined by plotting the known concentration, s_a, and drawing a straight line through this point at a slope determined from -15t. Thus, a measurement of sediment concentration at a known depth in the vertical section will allow its determination at any depth, provided the sediment composition is constant.

Another technique which is of practical value is the use of Manning's equation to solve for $\bar{V}$ in von Karman's universal velocity defect law, Equation (10). Using Manning's equation,

$$Q = \frac{1.5}{n} AR^{2/3} S_e^{1/2}, \tag{27}$$

where Q is the discharge and n is Manning's roughness coefficient (Chow, 3), in Equation (10) the quantity

$$\frac{\sqrt{gdS_e}}{k\bar{V}} = \frac{9.64}{d^{1/6}} n. \tag{28}$$

τ_o may also be determined directly from the velocity defect law by taking two point-velocities, inserting each into separate equations (Equation (10)) arranged to solve for $\bar{V}$. As the right sides of the equations are equal, they may be used to solve for τ_o, i.e.,

$$\tau_o = \rho \left[\frac{(V_2 - V_1)k}{\ln(\frac{y_2}{y_1})} \right]^2, \tag{29}$$

where V_1 and V_2 are the point velocities in the two equations, respectively. If k is 0.4 and the natural logarithm is converted to a common logarithm,

$$\tau_o = \rho \left[\frac{V_2 - V_1}{5.75 \log_{10}(\frac{y_2}{y_1})} \right]^2. \tag{30}$$

Although the above discussion represents the physical laws controlling the distribution of suspended sediment over the vertical cross section of a stream, it does not supply the complete solution to the problem, for s_a must be known for any information to be determined about the total sediment discharge.

Rainfall and Sediment Transport

Rainfall on a channel has been considered with respect to its effect on both the bedload and the suspended load. The effect of rainfall has been expressed with reference to its effect on the average velocity of flow and the velocity gradient (5). The effect on the velocity gradient will affect the tractive force at the channel bottom if the assumptions in von Karman's velocity defect law are valid. Flume studies by Smerdon (14) indicated that the critical tractive force, that is, the tractive force which causes significant scour of an erodible bed, was increased slightly by rainfall due to a reduction of shear at the bottom of the channel. He attributed this reduction of shear to the exchange of momentum from the flow to the raindrops in the upper zone affected by raindrop penetration.

Glass (5) substantiated Smerdon's findings by conducting tests on the velocity distribution in shallow channel flows, with and without simulated rainfall. His analysis consisted of a comparison of regression lines of the velocity distribution profile with and without rainfall.

Critical tractive forces were related to rainfall by Bathke (1), who found that no consistent relation existed between rainfall and channel erosion. However, his findings were not conclusive due to problems in the sediment sampling equipment, which were discovered after his tests were completed.

This literature indicates that rainfall has an effect on shallow flows, but its extent and description have not been determined. Furthermore, the instrumentation required to observe changes in sediment transportation requires additional study and refinement.

CHAPTER II

EQUIPMENT AND PROCEDURES

Equipment

The data for this study were collected in the Soil and Water Research Laboratory of the Agricultural Engineering Department. A research flume, Figure 2, equipped for recirculation of flow was used. The flume was 66 feet long, 2.5 feet wide, and 1.3 feet deep. The lower end of the flume was supported on a pivot, and the upper end was supported by a pair of hydraulic jacks. This arrangement allowed the upper end to be raised for any desired slope. The sides and bottom were constructed of 3/4-inch marine plywood with a 1/32-inch plastic veneer on each side. A plexiglass section in the sides at a distance of 18 to 42 feet from the upstream end was included to permit observation of the flow (Figure 3). An adjustable slatted gate located at the lower end of the flume was used to control flow to approximate uniform flow conditions (Figure 2).

The flow entered the flume through an 8-foot transition nozzle constructed of 3/4-inch plexiglass. In the 8-foot length, the width increased from 0.5 feet to 2.5 feet, and the height increased from 0.5 feet to 1.3 feet (Figure 4). The nozzle was designed to permit a smooth transition of the flow from the entrance pipe to the flume section.

Figure 2. Recirculation Flume Viewed from the Side.

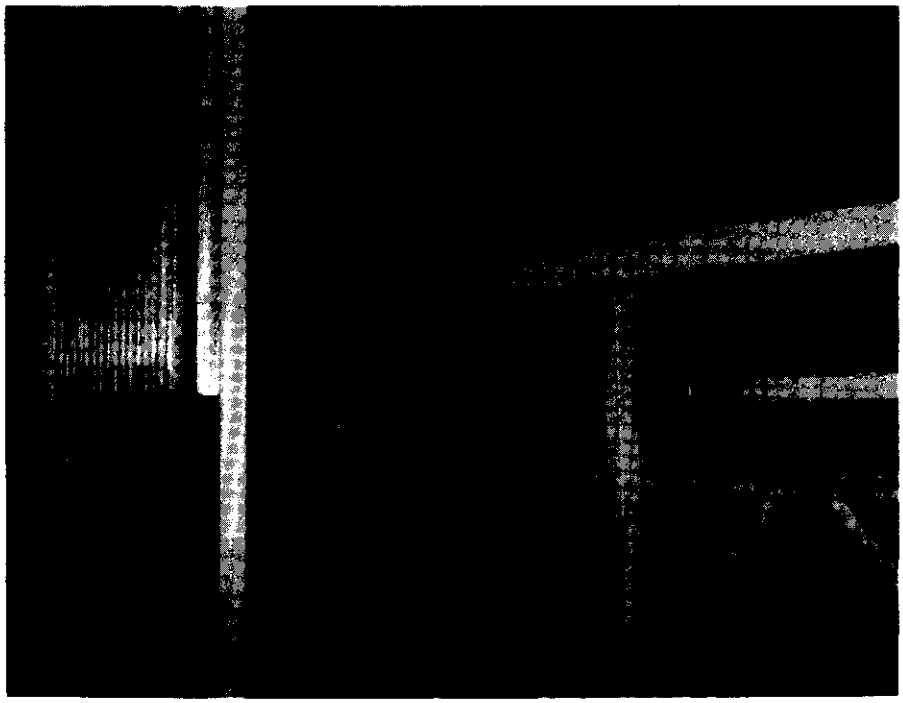

Figure 3. Plexiglass Side Section and Manometer Board.

Figure 4. Transition Nozzle at Flume Inlet and Centrifugal Rainfall Simulator Pump.

Although this nozzle prevented the flow from separating from the bottom and sides of the flume, it did not allow for sufficient energy dissipation to prevent a hydraulic jump from occurring in the test section downstream. Therefore, a baffle in the nozzle was necessary to force the hydraulic jump to form in the nozzle or immediately downstream. Otherwise, supercritical velocity flow would have extended through much of the flume length before the hydraulic jump occurred. The desired flow condition in the flume was at subcritical velocity (tranquil flow).

The flow from the flume discharged into a 5.5-feet wide, 8.7-feet long, and 3.5-feet deep steel tank, whose bottom was sloped toward a slotted intake pipe to the recirculation pump. This system allowed the flow to be taken from the entire length of the tank and permitted a minimum of sediment to collect at the bottom of the tank.

Water was recirculated by a centrifugal pump which pumped from the catch tank through a 6-inch pipe to the flume inlet (Figure 5). This flow through the flume was regulated by a gate valve.

The flume was equipped with a special rainfall simulator which used 12 Spraying Systems Company 80100 Veejet nozzles to simulate rainfall. These nozzles were spaced along a 1-inch pipe extending the length of the flume at a height of 8 feet above the center of the flume floor. The simulator design was based on rainfall simulator research conducted by Meyer and McCune (10) and resulted in the following characteristics of the simulated rainfall:

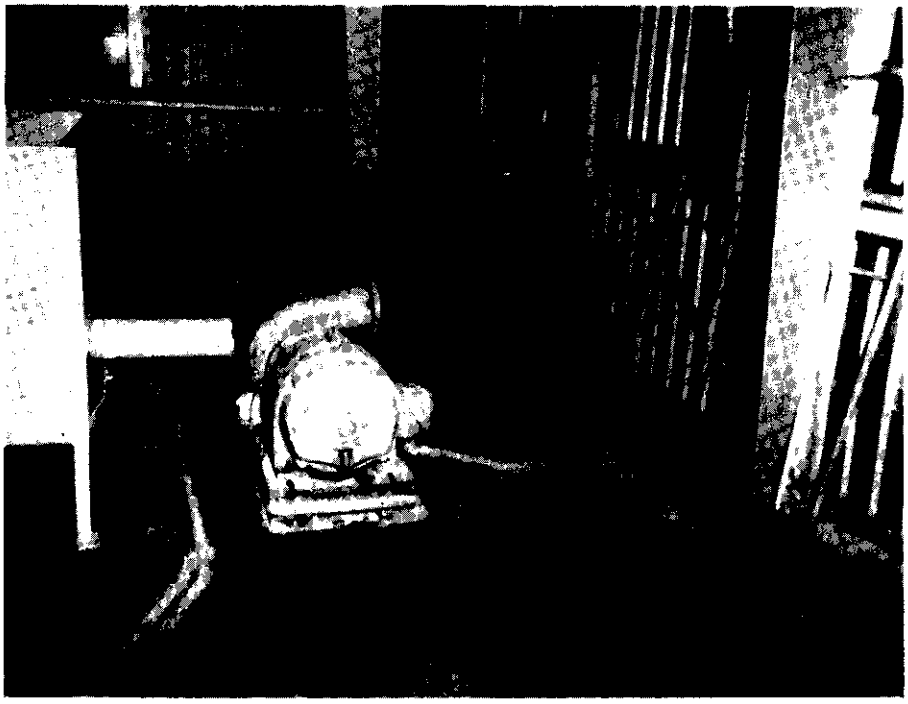

Figure 5. Centrifugal Recirculation Pump with a Capacity of 1500 gpm.

1. A drop size distribution that was similar to that of natural rainfall.
2. A drop fall velocity that was near the terminal velocity of raindrops, which is from 16 to 30 feet per second for drop diameters of 1.25 to 6.00 millimeters.
3. A high degree of longitudinal uniformity along the flume.
4. A rainfall intensity that could be maintained at a desired level.

The simulator was supplied with water taken from a point near the upper end of the 6-inch return pipe by a 3/4-inch centrifugal pump (Figure 4). This arrangement was selected because sediment-ladened rainfall was desired to prevent dilution of the flume flow. Flow in the return pipe was selected because it represented the average sediment concentration of the flow under equilibrium conditions. Also, a constant total flow was necessary before and after rainfall. Therefore, the rainfall had to be taken from the flow near the outlet of the return pipe to allow the flume recirculation pump to work against a constant head, regardless of whether rainfall was being simulated. The simulator pump was attached to a 1.5-inch pipe extending the length of the flume. The flow was transferred to the overhead simulator line by four evenly spaced 1-inch rubber hoses, which provided a uniform pressure at the nozzles.

The system was equipped with instrumentation to measure total flow, point velocities, the water surface profile with respect to the bottom of the flume and the horizontal, point sediment concentrations, average concentrations, rainfall intensity, and temperature.

Total flow was measured by an H-type flume with a water level recorder which was used to calibrate a Dall flow nozzle. The Dall nozzle was connected to two well-type manometers, one with indicating fluid (specific gravity—1.75) and the other with mercury (specific gravity—13.55). The manometers were checked for proper calibration by comparing them with the calibrated H-type flume, which was not subsequently used. The mercury manometer proved to be the more desirable, as the fluctuations of the indicating fluid made accurate readings difficult.

Point velocities were taken with a Prandtl tube having a velocity coefficient of 1.0 (Figure 6). The Prandtl tube was mounted on a threaded shaft and a track placed perpendicular to the flow. This arrangement allowed point velocities to be taken at any point in a cross section of the flow. The total and static head lines from the Prandtl tube were connected to a differential inclined manometer having a multiplication factor of four (Figure 7). The manometer allowed the velocity head to be read directly. Point velocities in feet per second were determined by the following modification of the velocity head equation,

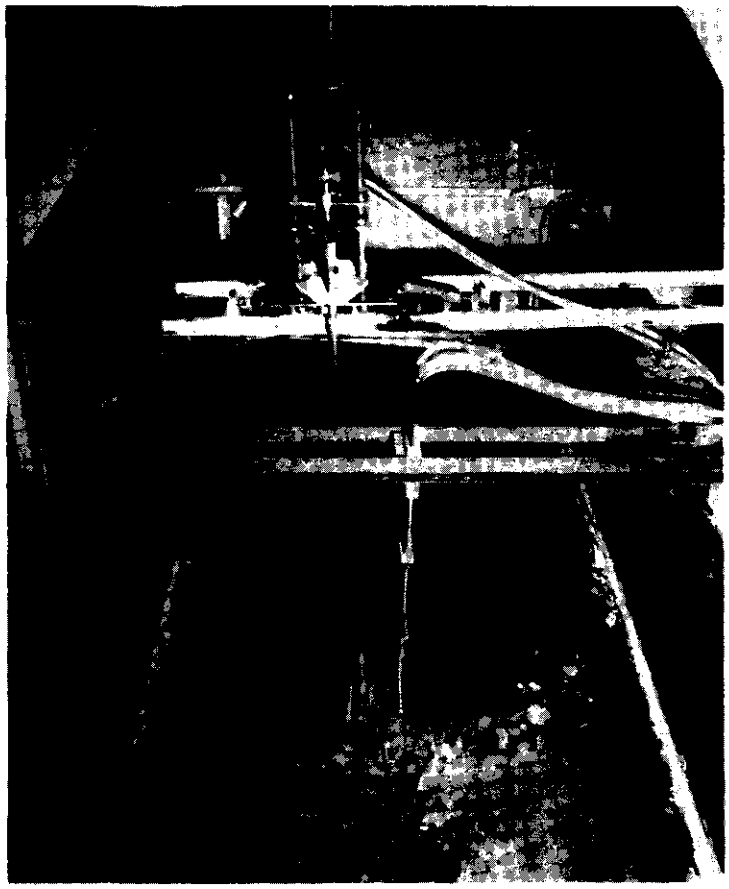

Figure 6. Prandtl Tube (in rear) and Suspended Sediment Sampling Tubes (in foreground).

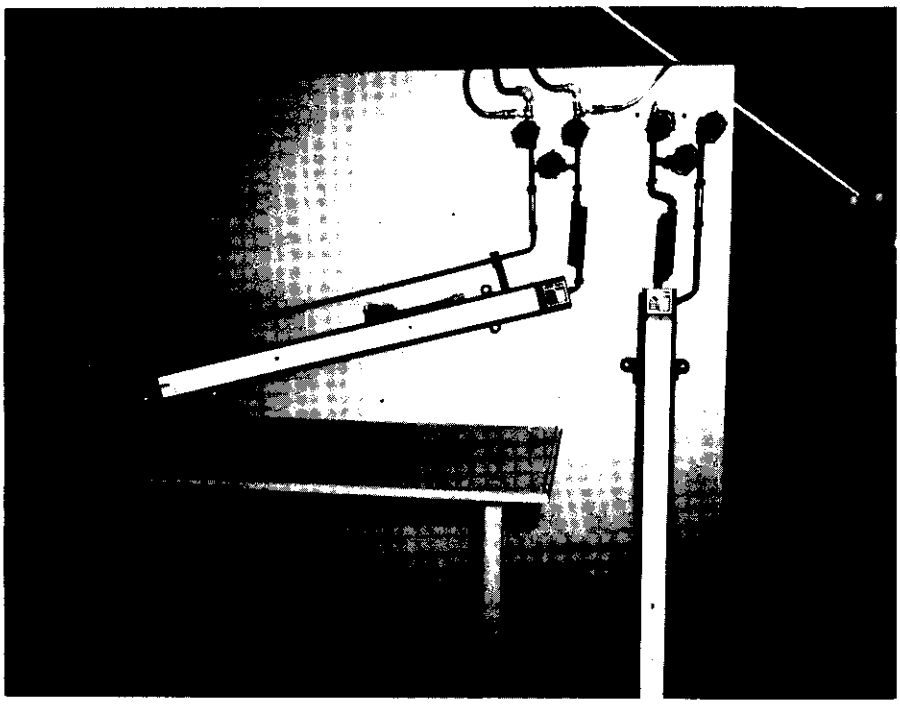

Figure 7. Differential Inclined Manometer.

$$V = \sqrt{\frac{gh}{8}} = 2\sqrt{h}, \qquad (31)$$

where h is the height of the manometer fluid (Specific gravity—1.75) in inches.

The water surface profile was obtained with respect to the flume bottom from four manometer tubes attached to the side of the flume at intervals of 6 feet. The surface profile with respect to the horizontal was taken from a manometer board connected to 16 piezometer orifices spaced along the length of the flume and connected to the board with transparent Tygon tubing (Figure 6). The upstream piezometer orifice was located 4 feet from the upstream end of the flume. The four upstream piezometer orifices were 6 feet apart, the next nine were 3 feet apart, and the last four were 6 feet apart. The last four were attached to the piezometer orifices of the four manometers previously described.

Suspended sediment concentration in the flow was determined by analyzing 10 milliliter samples with a Klett-Summerson photoelectric colorimeter (6,15). The colorimeter (Figure 8) operated on a potentiometric principle, using a light source, two matched photoelectric cells, a potentiometer, and a galvanometer. Operation of the colorimeter consisted of obtaining a null reading on the galvanometer by adjusting the scale on the potentiometer to a logarithmic number.

Point samples of sediment were taken from four 3/16-inch L-shaped sediment sampling siphon tubes (Figure 6), whose siphoning

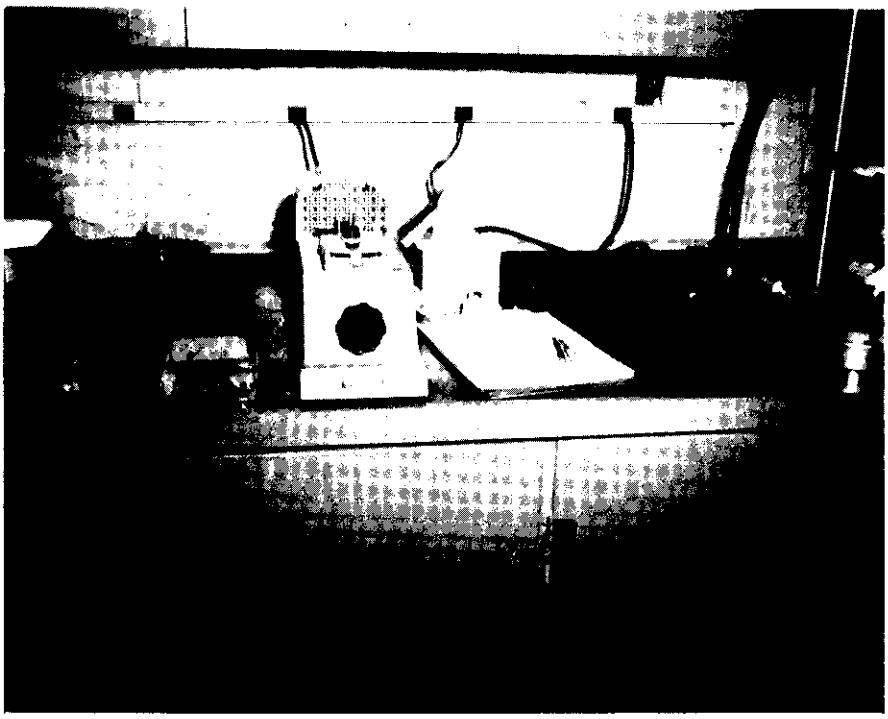

Figure 8. Klett-Summerson Photoelectric Colorimeter.

head was adjusted so that the velocity of flow into the samples was approximately equal to the flow in the flume at the sampling point. The samples for determining total sediment were taken from a slit sampler at the lower end of the flume. The slit was approximately 6 inches long and 1/16-inch wide (Figure 9). Pint samples were taken for the total sediment load analysis. These samples were taken by traversing the width of the flume at the apron which carried the flow to the catch tank. The flow on the apron was supercritical, and the edges of the slit were sharpened. This permitted samples representative of the total load to be taken.

The rainfall intensity pattern (Figure 10) was determined for different operating conditions of the simulator by taking volumetric samples over a section of the flume bottom. The total flow from a nozzle at a pressure of 8 psi was then compared to that of 5 psi to obtain the rainfall intensity at both levels. Temperature was measured by placing a standard mercury thermometer in the flow.

Sediment Characteristics

Preliminary tests were conducted with natural sediment which was collected in preweighed bottles, transferred to beakers weighed to $\pm$ 0.5 milligrams, oven-dried, reweighed, and corrected for the dissolved soils in the water. The weights were taken under conditions of constant temperature and humidity.

Figure 9. Operation of the Total Load Sediment Sampler.

o - Sprinkler
Scale - 1" = 1'
High Rainfall Intensity = Low x 1.5
Isolines are in Inches per Hour

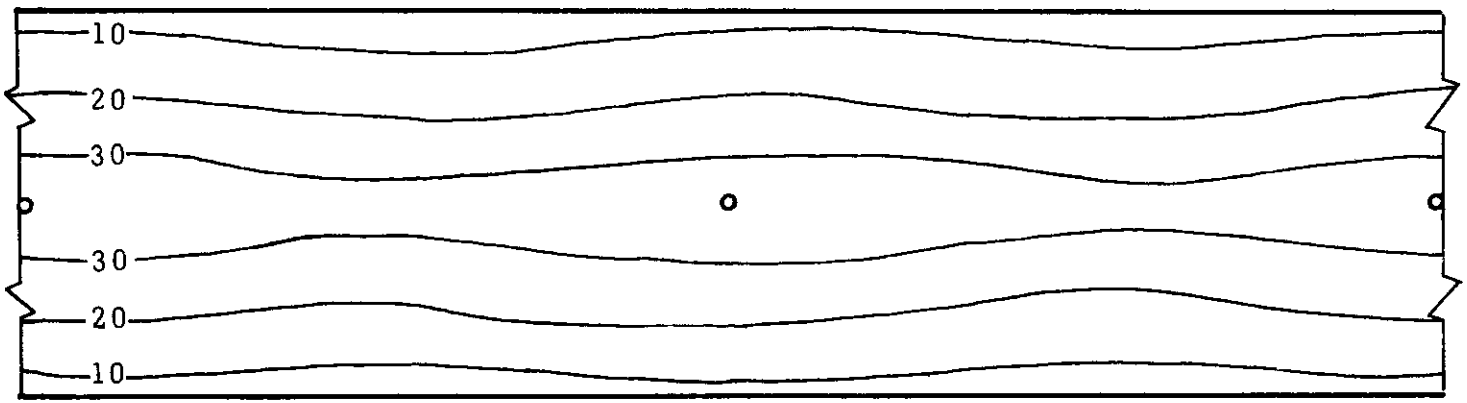

Figure 10. Plan View of Rainfall Distribution in Flume for Low Rainfall Intensity.

However, no significant differences were observed in the sediment load at various depths as a result of simulated rainfall. A study of the particle sizes of the soil sample used indicated a size distribution of 53.8 per cent sand, 24.7 per cent silt, and 21.6 per cent clay. Sand was defined as sediment having particle diameters greater than 0.05 millimeters, silt, 0.002-0.05 millimeters, and clay, less than 0.002 millimeters. Because the sediment in the sand range rapidly settled out and the colloidal sized clay remained in suspension regardless of the flow conditions, a sediment consisting of only particles in the silt range was selected for these studies.

Spherical glass beads in the silt size range were ultimately chosen to simulate sediment. Figure 11 is a photomicrograph of the glass beads. These were commercial beads having the following specifications:

1. Median diameter—29 microns (0.0011 inches).
2. Specific gravity—1.45.
3. Optical properties—colorless optical lenses which refracted light in a manner to permit a large percentage to be returned toward the source.
4. Shape—3 to 10 per cent were not accurate spheres.
5. Size range—18 to 40 microns (approximately 90 per cent by weight within the specified size range, less than one per cent by weight finer than 0.0007 inches).

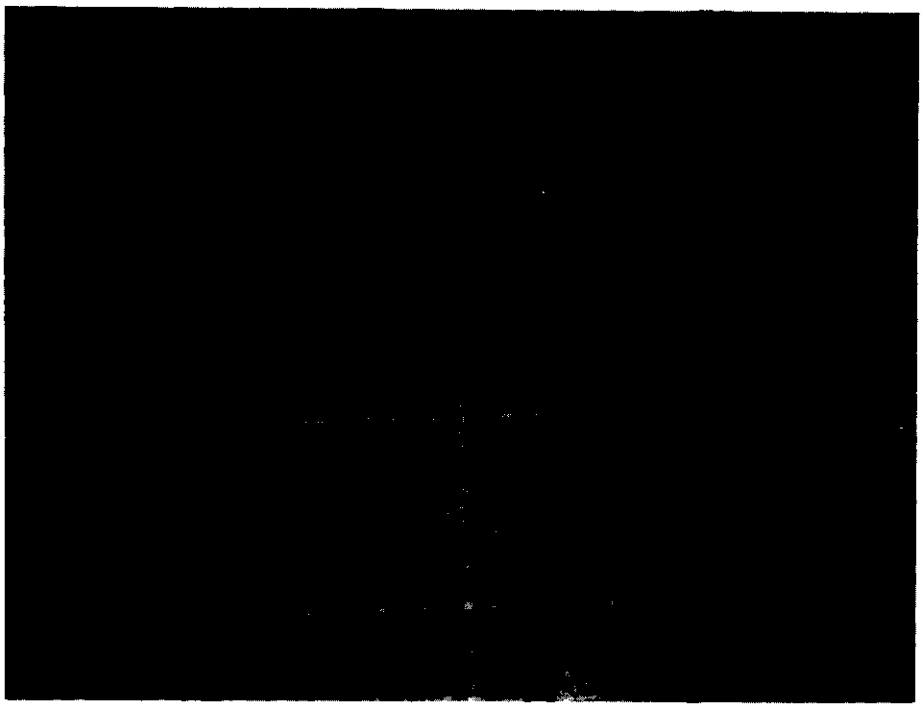

Figure 11. Photomicrograph of Glass Beads. (Sides of small squares are 40 microns in length.)

6. Fall velocity (Stokes' Law for 80°F.)

   a. 18 microns—0.00102 feet per second

   b. 29 microns—0.00259 feet per second

   c. 40 microns—0.00495 feet per second

Procedures

The procedure for this study involved a design which would permit the effect of the rainfall on sediment transport for a given set of flow conditions to be determined (19). Therefore, a set of uniform flow conditions was established for the flume by adjusting the slope, discharge, and tailwater board. Once uniform flow was established, glass beads were added to the flow until they were observed forming dunes on the floor of the flume (Figure 19). Then, all flow conditions were recorded and a velocity profile was made at the point where the sediment samples were to be taken. The Prandtl velocity tube was then removed from the flow, and the sediment sampling tubes were emplaced. A depth of flow of 0.35 feet was used and four sampling depths were selected at 0.32 feet, 0.22 feet, 0.12 feet, and 0.02 feet.

Sediment samples were collected as follows: Ten milliliter samples from each of the four point samplers and the total load sampler were collected in test tubes at 2-minute intervals for a 30-minute period. At the end of this period, the simulated rainfall was started. As previously stated, the rainfall was taken from the total flow, so

the discharge at the end of the flume was unchanged, and the existing flow was not diluted. A period of four minutes was allowed for the system to re-establish equilibrium, with the rainfall of a given intensity being the only imposed difference. Then samples with rainfall were collected by the same procedure. At the end of the test, 16 samples without and 16 samples with rainfall had been collected from each of the four point samplers and the total load sampler.

The experimental design required data to be collected for two velocities and two rainfall intensities with two replications of each set of conditions, for a total of eight runs. After samples from a run had been taken, they were analyzed as follows. Each 10 milliliter sample was agitated to bring the sediment into suspension, transferred to one of a set of matched tubes for use with the colorimeter, reagitated, and then analyzed with the colorimeter, using distilled water for a zero setting.

In order for the colorimeter readings to be converted to sediment concentrations, the colorimeter was calibrated by accurately weighing samples of sediment and establishing known concentrations. These samples were then tested, and a calibration curve was constructed (Figure 12). (This curve did not follow Beer's Law, which states that the amount of light absorbed by a solution is directly proportional to the concentration of the substance in solution absorbing the light, as a solution was not being studied.) However, the curve was constructed

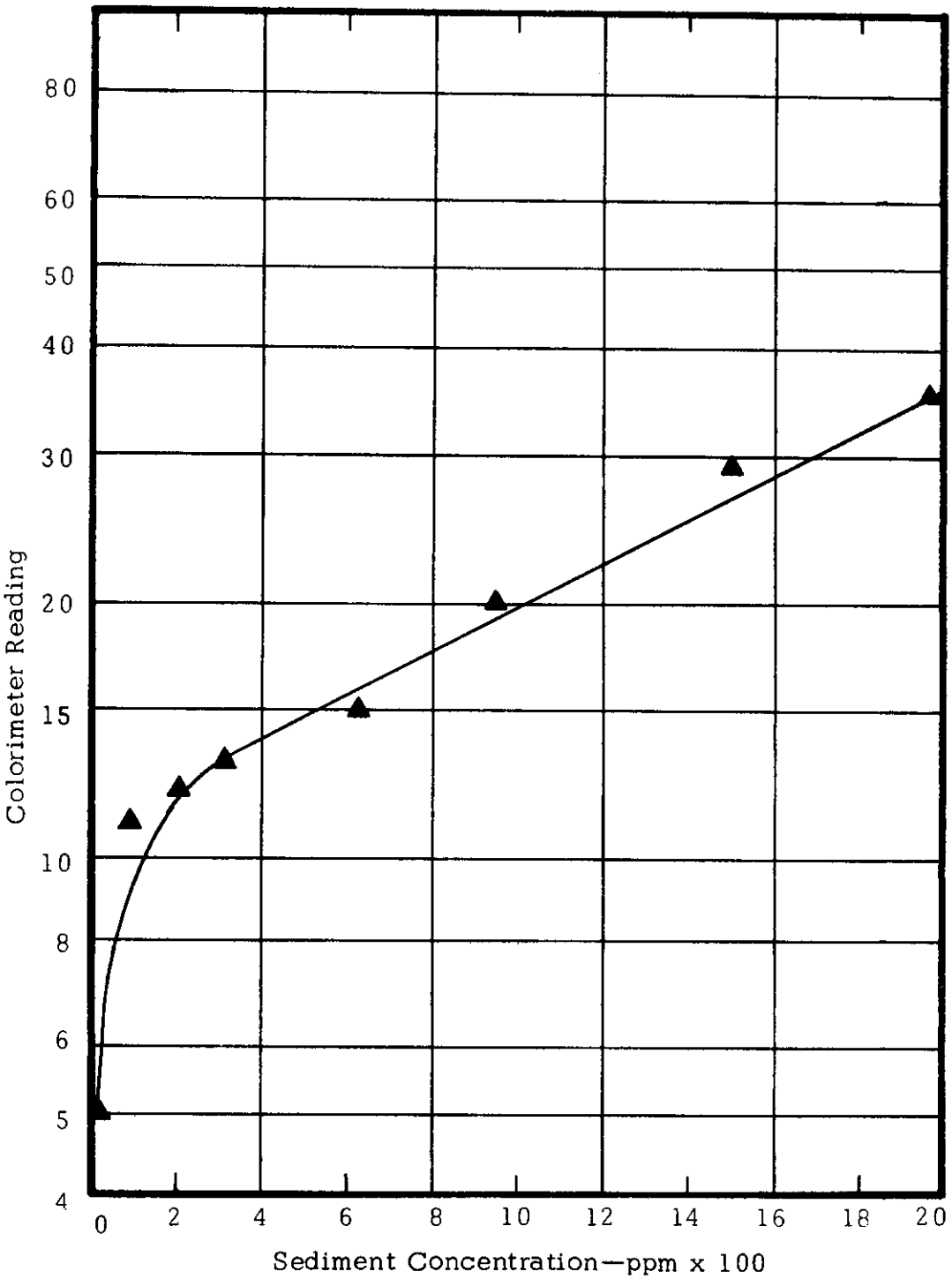

Figure 12. Calibration Curve for Colorimeter.

on semi-logarithmic paper by plotting the logarithmic colorimeter readings on the logarithmic scale versus concentrations on the linear scale. A straight line was obtained except at very low concentrations.

Preliminary studies indicated more scatter in the samples than could be attributed to sampling error. Therefore, 21 samples were taken from an apparent homogeneous sample drawn from the total flow sampler. An analysis of these samples indicated a variance less than was obtained during the tests. As a result, an analysis of variance was made to determine the effects of rainfall and flow velocity on variance.

Further studies were then conducted to determine the two levels of velocity and rainfall intensity to be used during the tests. The minimum velocity at which the bulk of the sediment could be held in suspension was approximately 1.2 feet per second; therefore, the low velocity level was selected at approximately 1.5 feet per second. For near uniform flow, the maximum subcritical velocity which could be obtained at the depth of 0.35 feet was approximately 1.8 feet per second. This velocity was selected as the high velocity level.

The two levels of rainfall were chosen at five and eight psi, which corresponds to an intensity at the center of the flume of approximately 35 inches per hour at five psi and 50 inches per hour at eight psi. Unusually high rainfall intensities were used to magnify small changes in flow conditions which might result from rainfall.

CHAPTER III

ANALYSIS OF DATA AND DISCUSSION OF RESULTS

Data Analaysis

The experiment was designed primarily to determine if changes in the suspended load or total sediment load could be attributed to the effects of rainfall. Therefore, flow conditions were established and a statistical analysis was selected accordingly.

Suspended sediment concentration was measured at four depths in the vertical profile. The total load was examined to determine if the suspended load was evenly distributed over the width of the flow profile. Also, a study of the total load was necessary to determine if changes in suspended load due to simulated rainfall were transported as bedload.

The data were analyzed statistically by use of analysis of variance techniques (9). The first portion of the statistical analysis consisted of an analysis of the variance of the common logarithms of the colorimeter readings from the final 13 samples from each sampling point taken before and after rainfall. (The first three samples of the 16 taken at each point for each condition were not used because the system required 10 minutes to reach equilibrium instead of the four allowed)(Table 1). This analysis of variance was performed on the two replications of the two velocity and rainfall levels at each depth and for the total load to determine if a change in the variances was due to these variables. The logarithms of the

Table 1. Analysis of Variance for the Common Logarithms of the Variances

Source of Variance	Sums of Squares	Degrees of Freedom	Mean Square
	y = 0.32 foot		
Between Runs	0.2932	7	
Low versus High Velocity	0.0473	1	0.0473
Error (a)	0.2459	6	0.0410
Within Runs	1.0953	8	
No Rain versus Rain	0.2176	1	0.2176
Interaction	0.0088	1	0.0088
Error (b)	0.8689	6	0.1448
	y = 0.22 foot		
Between Runs	0.2050	7	
Low versus High Velocity	0.0023	1	0.0023
Error (a)	0.2027	6	0.0338
Within Runs	0.5442	8	
No Rain versus Rain	0.0807	1	0.0807
Interaction	0.2642	1	0.2642*
Error (b)	0.1993	6	0.0332

* Significant at the 5% level.

Table 1 (cont'd)

Source of Variance	Sums of Squares	Degrees of Freedom	Mean Square
	y = 0.12 foot		
Between Runs	0.2544	7	
Low versus High Velocity	0.0061	1	0.0061
Error (a)	0.2483	6	0.0414
Within Runs	0.4375	8	
No Rain versus Rain	0.1582	1	0.1582
Interaction	0.0321	1	0.0321
Error (b)	0.2472	6	0.0412
	y = 0.02 foot		
Between Runs	0.7569	7	
Low versus High Velocity	0.3703	1	0.3703
Error (a)	0.3866	6	0.0644
Within Runs	0.4066	8	
No Rain versus Rain	0.1096	1	0.1096
Interaction	0.0098	1	0.0098
Error (b)	0.2872	6	0.0479
	Total Flow		
Between Runs	0.3560	7	
Low versus High Velocity	0.0539	1	0.0539
Error (a)	0.3021	6	0.0504
Within Runs	0.2848	8	
No Rain versus Rain	0.0012	1	0.0012
Interaction	0.1049	1	0.1049
Error (b)	0.1787	6	0.0298

variances of the colorimeter readings were used according to a modified method of Bartlett's statistic (Li, 9).

The second portion of the statistical analysis involved the same procedure except the means of the 13 colorimeter readings were used rather than their variances (Table 2). The purpose of this analysis was to determine the effect on the sediment concentration due to rainfall or velocity at each of the four sampling depths and for the total flow.

Variation of Sediment Samples

The computations of variances in sediment concentration indicated no significant difference in the variances due to rainfall or velocity, except that the sampler at a distance of 0.22 feet above the flume bottom revealed an interaction significance at the five per cent level (Table 1). The variance of the means revealed an increase in the sediment concentration due to an increase in velocity significant at near the one per cent level (Table 2). A significant change in the total load concentration due to rainfall was observed at the one per cent level. However, no significant change in sediment concentration was evident at any of the four point samplers.

The fact that the variances were not affected by rainfall or velocity indicates that there were no noticeable changes in the fluctuations in sediment concentration. The significance in the previous interaction was attributed to the low sum of squares obtained for low versus high

Table 2. Analysis of Variance for the Means of the Colorimeter Readings

Source of Variance	Sums of Squares	Degrees of Freedom	Mean Square
	y = 0.32 foot		
Between Runs	130.00	7	
Low versus High Velocity	90.25	1	90.25**
Error (a)	39.75	6	6.62
Within Runs	26.00	8	
No Rain versus Rain	6.25	1	6.25
Interaction	9.00	1	9.00
Error (b)	10.75	6	1.79
**Significant at the 1.0% level.			
	y = 0.22 foot		
Between Runs	255.00	7	
Low versus High Velocity	196.00	1	196.00**
Error (a)	59.00	6	9.83
Within Runs	20.00	8	
No Rain versus Rain	1.00	1	1.00
Interaction	4.00	1	4.00
Error (b)	15.00	6	2.50
** Significant at the 1.0% level.			

Table 2 (cont'd)

Source of Variance	Sum of Squares	Degrees of Freedom	Mean Square
	y = 0.12 foot		
Between Runs	303.50	7	
Low versus High Velocity	203.00	1	203.00*
Error (a)	100.50	6	16.75
Within Runs	19.50	8	
No Rain versus Rain	1.75	1	1.75
Interaction	1.50	1	1.50
Error (b)	16.25	6	2.71
	y = 0.02 foot		
Between Runs	209.94	7	
Low versus High Velocity	138.19	1	138.19*
Error (a)	71.75	6	11.96
Within Runs	16.50	8	
No Rain versus Rain	1.56	1	1.56
Interaction	0.44	1	0.44
Error (b)	14.50	6	2.42

* Significant at the 5.0% level.

*Significant at the 5.0% level.

Table 2 (cont'd)

Source of Variance	Sums of Squares	Degrees of Freedom	Mean Square
	Total Load		
Between Runs	180.32	7	
Low versus High Velocity	115.94	1	115.94*
Error (a)	64.38	6	10.73
Within Runs	37.50	8	
No Rain versus Rain	21.82	1	21.82**
Interaction	6.31	1	6.31
Error (b)	9.37	6	1.56

* Significant at the 5.0% level.
** Significant at the 1.0% level.

velocity (Table 1), which was probably due to chance only.

Sample Means

The significant difference in the observation of the suspended sediment sample means at each sampling depth as affected by velocity is in agreement with O'Brien's equation, provided the following assumpations are made:

1. Von Karman's universal velocity defect law is valid, i.e., the velocity distribution is logarithmic with and without rainfall.
2. The shear is distributed linearly both with and without rainfall.
3. Von Karman's coefficient, k, is constant.

Figures 13-16 indicate that the velocity distribution is logarithmic both with and without rainfall. A comparison of the plots of the velocity profiles indicates only a slight change in the slopes of the curves. Since the slope of the velocity gradient, which is proportional to von Karman's coefficient did not change appreciably, the relative sediment concentration should be predictable by O'Brien's relationship for each condition. These tests showed that velocity has a highly significant effect on sediment transportation, therefore the sediment load should be reduced due to the noticeable decrease in velocity resulting from rainfall. However, this reduction was of such a magnitude that any reduction in the sediment load went unnoticed due to the degree of colorimeter sensitivity, which allowed an error on the order of ± 50 ppm.

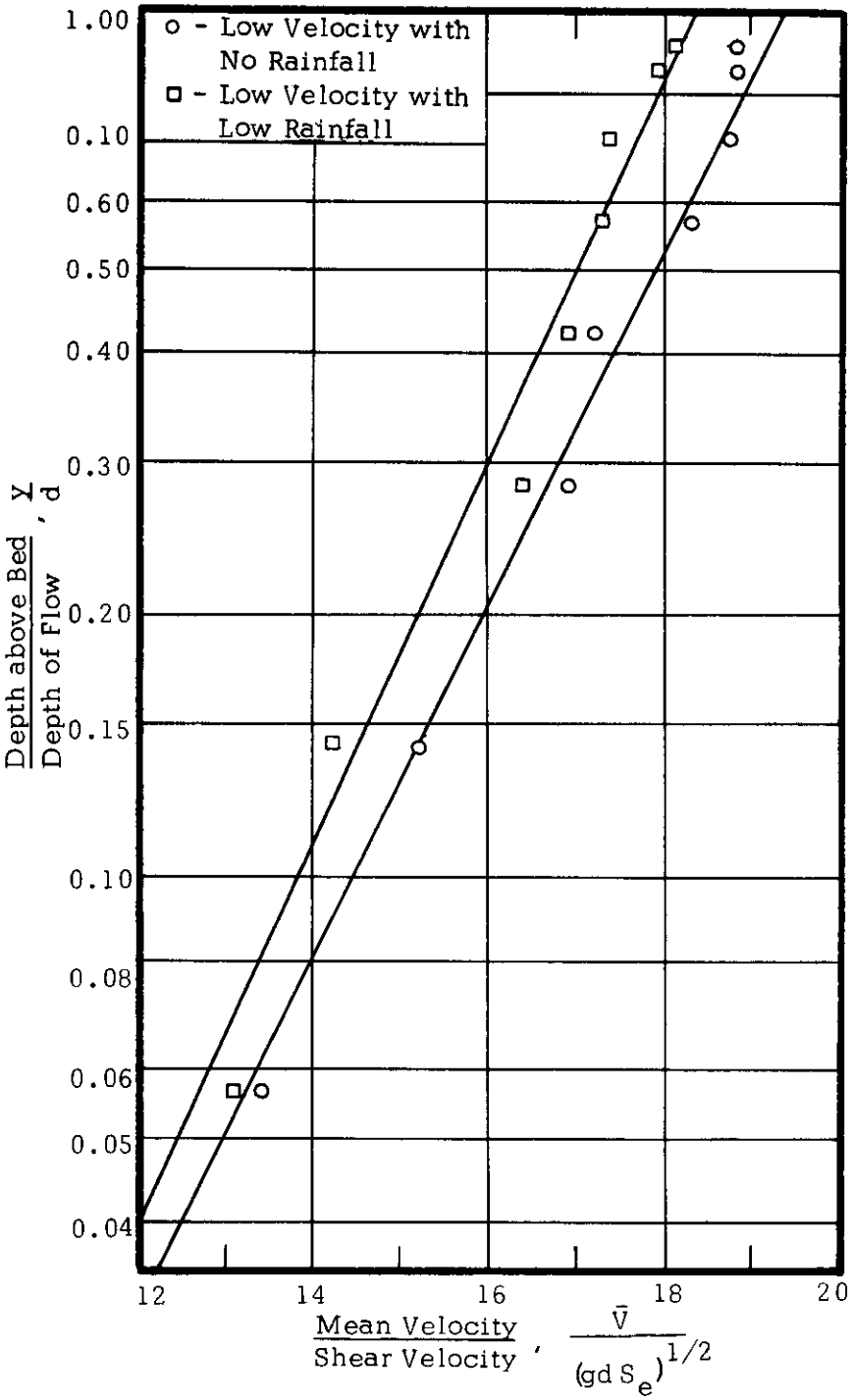

Figure 13. Velocity Distribution Curves Comparing Low Velocity without Rainfall to Low Velocity with Low Rainfall Intensity.

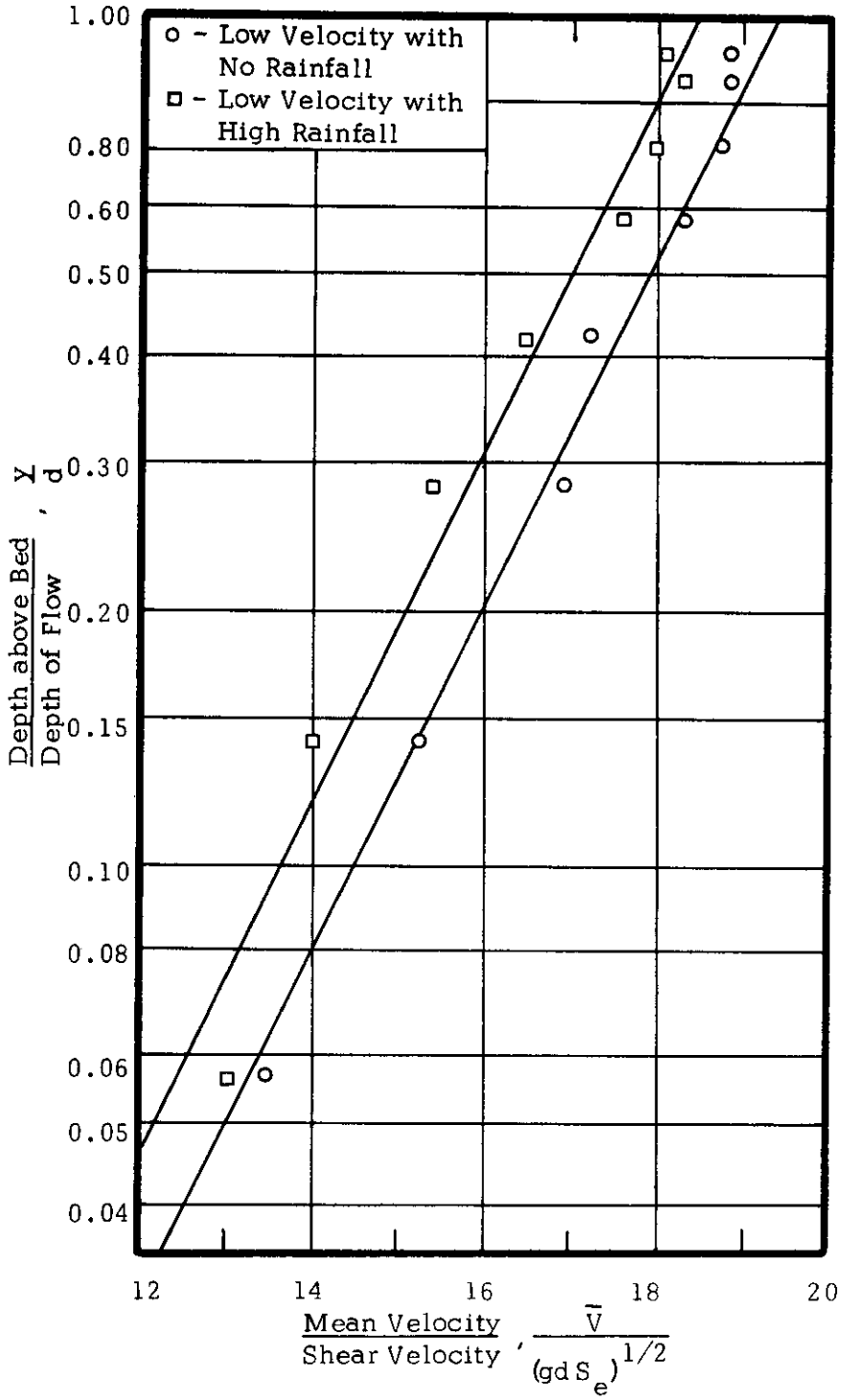

Figure 14. Velocity Distribution Curves Comparing Low Velocity without Rainfall to Low Velocity with High Rainfall Intensity.

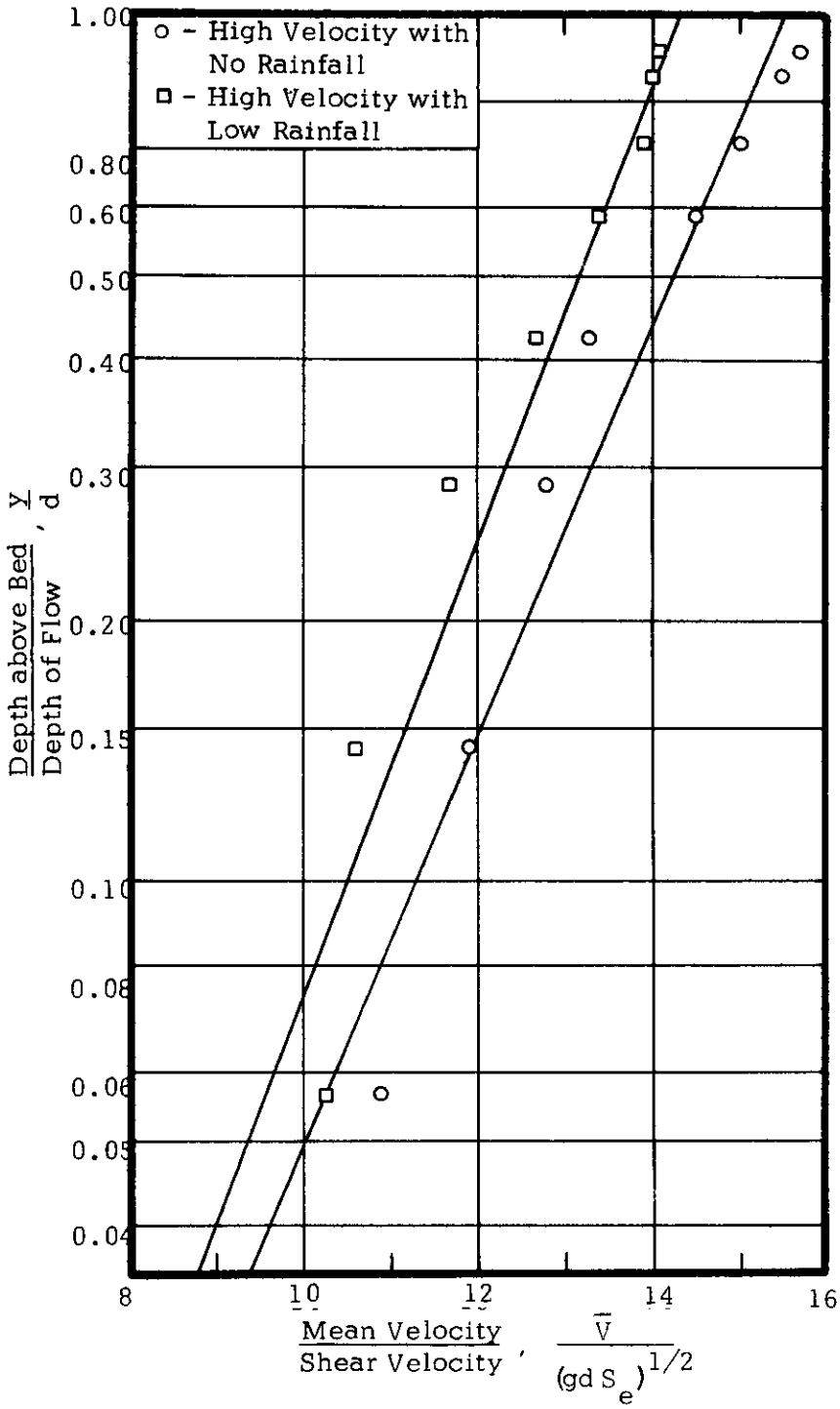

Figure 15. Velocity Distribution Curves Comparing High Velocity without Rainfall to High Velocity with Low Rainfall Intensity.

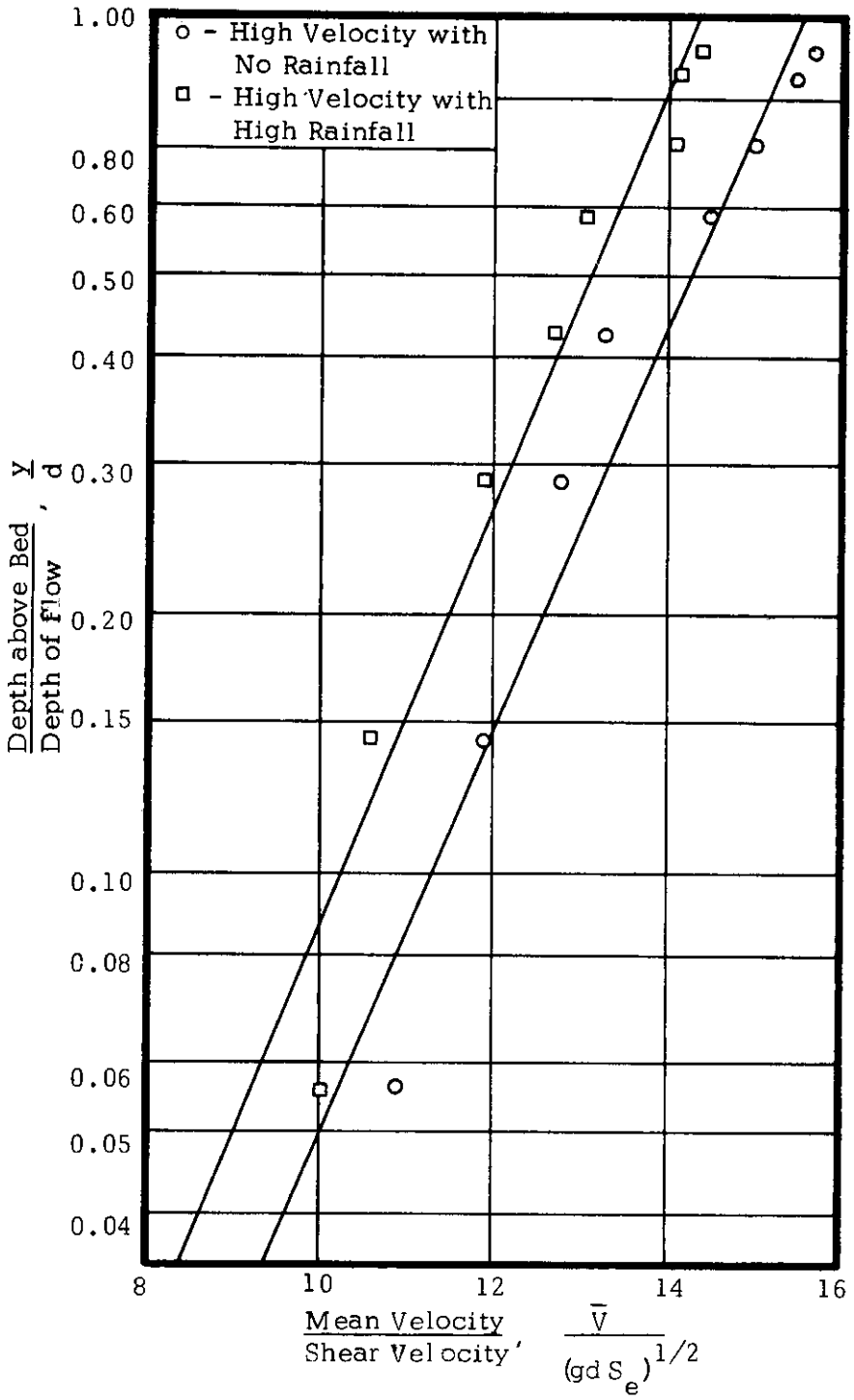

Figure 16. Velocity Distribution Curves Comparing High Velocity without Rainfall to High Velocity with High Rainfall Intensity.

Determination of Shear

Plots of the velocity distributions could not be made directly for all flow conditions. Since the abscissas of the plots involved the shear velocity, V_*, the slope of the energy grade line had to be estimated for the high velocity flows, whereas the slope of the channel was used for low velocity flow. The slope of the channel was calculated from equal readings of the four manometers located on the side of the flume and the slope indicated on the manometer board. The slope for high velocity flow was estimated by computing values for von Karman's coefficient and Manning's roughness coefficient for low velocity flow and applying these values to high velocity conditions. Also, calculations for nonuniform flow at high velocity conditions were made.

The slope at low velocity was computed as 0.0007 from the slope of the water surface taken from the manometer board. τ_o at the sediment sampling point was determined as:

$$\tau_o = \gamma d S_e \qquad (4)$$

$$\tau_o = (62.4)(0.35)(0.0007) = 0.0146 \text{ lb/ft}^2.$$

Von Karman's coefficient was then determined by selecting two point velocities from the logarithmic velocity distribution curve and solving for k as follows:

$$\tau_o = \rho\left[\frac{(V_2-V_1)k}{2.3\log_{10}(\frac{y_2}{y_1})}\right]^2 ; \qquad (29)$$

when $y_2 = 0.8d$ and $y_1 = 0.2d$,

$$k = \sqrt{\tau_o}/V_2-V_1 = \sqrt{0.0146}/0.26 = 0.47.$$

Manning's n was then determined for low velocity flow as follows:

$$Q = \frac{1.5}{n} AR^{2/3}S_e^{1/2} \qquad (27)$$

$$1.2 = \frac{1.5}{n} (.876)(.27)^{2/3}(.0007)^{1/2}$$

$$n = 0.012.$$

The calculated k and point velocities at known depths were used in Equation (29) to determine a value of τ_o equal to 0.0186 pounds per square foot for high velocity flow. Then Equation (4) was used to determine S_e equal to 0.0009. The computed Manning's n and a discharge of 1.36 cubic feet per second also resulted in a computed S_e of 0.0009 from Equation (27). A more direct method of computing the slope for nonuniform flow involves a consideration of the force parallel to the channel bed which is a result of acceleration or deceleration of the flow. Chow (4) has derived a tractive force equation for nonuniform flow, which is

$$S_e = (\frac{q^2}{gd^3} - 1)\frac{dd}{dx} + S_o , \qquad (32)$$

where q is the discharge per unit width of channel, and dd/dx is the change in depth. This equation gave S_e equal to 0.0012. Since the first two procedures involved a calculated value for k and n, respectively, the value of S_e from Equation (32) was considered the most accurate. Since S_e was necessary to compute the shear velocity, 0.0012 was used for the plots comparing the logarithmic velocity distributions for the various combinations of velocity and rainfall.

Velocity Considerations

An analysis of the velocity profile at the four combinations of velocity and depth confirmed the observations of Smerdon (14) and Glass (5) that the velocity gradient is logarithmic with and without rainfall. Figures 13-16 indicate a reduction in velocity at the center of the flume as a result of rainfall. This reduction was greater near the surface for the low intensity rainfalls, but for high intensities, the reduction was approximately the same throughout the profile.

The study of the velocity profile further revealed that the reduction in velocity near the center of the flume resulted in only very slight increases in depth. This can be explained by the fact that the addition of rainfall introduced spatially varied flow into the flume, but did not increase the total flow at the end of the flume. That is, the total flow with rainfall was lower at the upper end of the flume but increased to

the original discharge rate at the lower end of the flume. The maximum intensity of rainfall was along the centerline of the flume (Figure 10). As a result, flow was observed toward the sides of the flume (Figures 17 and 18) due to a higher rainfall intensity near the center of the flume and the reduction in velocity. The reduction in velocity due to rainfall can be explained by the conservation of momentum, because the momentum of the raindrops in the horizontal plane is zero. The increase in velocity near the flume sides resulting from rainfall was apparent throughout the profile, as the dunes of sediment were swept away from the flume walls out to a distance of approximately six inches (Figures 19 and 20).

This change of flow conditions is believed to be the explanation for the significant difference in total load. Since the total load was integrated over the width and depth, one consideration was to determine if this change in total load could be attributed to the change in flow conditions near the sides of the flume. Another was to determine if it were due to a change in the sediment transported as bedload, which could not be sampled by the point samplers. Therefore, this reduction in total sediment load was studied by taking a set of samples from the center and from the sides of the flume at conditions of low velocity and high

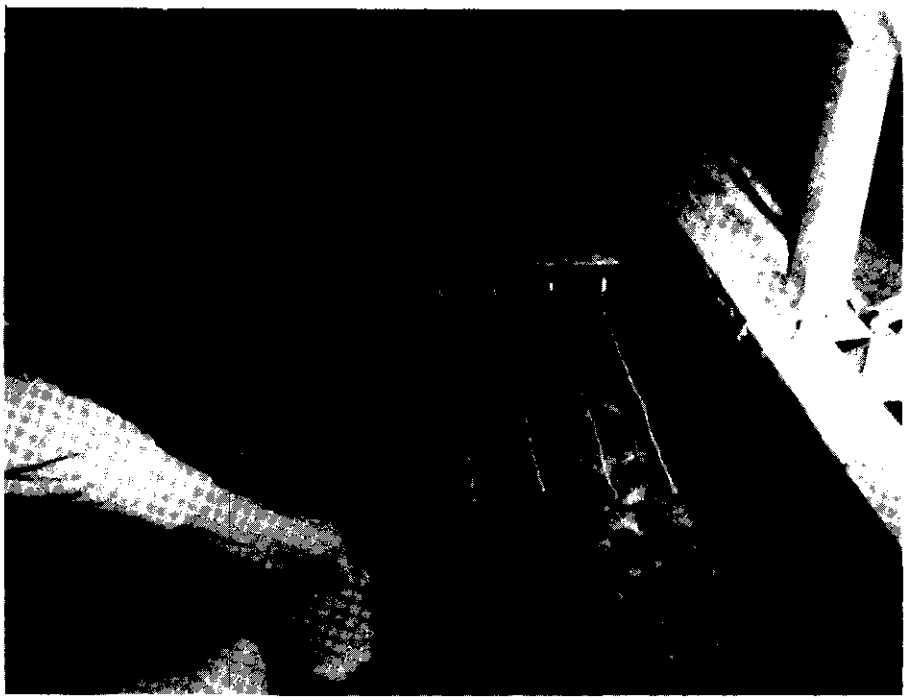

Figure 17. Strings Suspended in the Flow Showing the Direction of Flow without Rainfall.

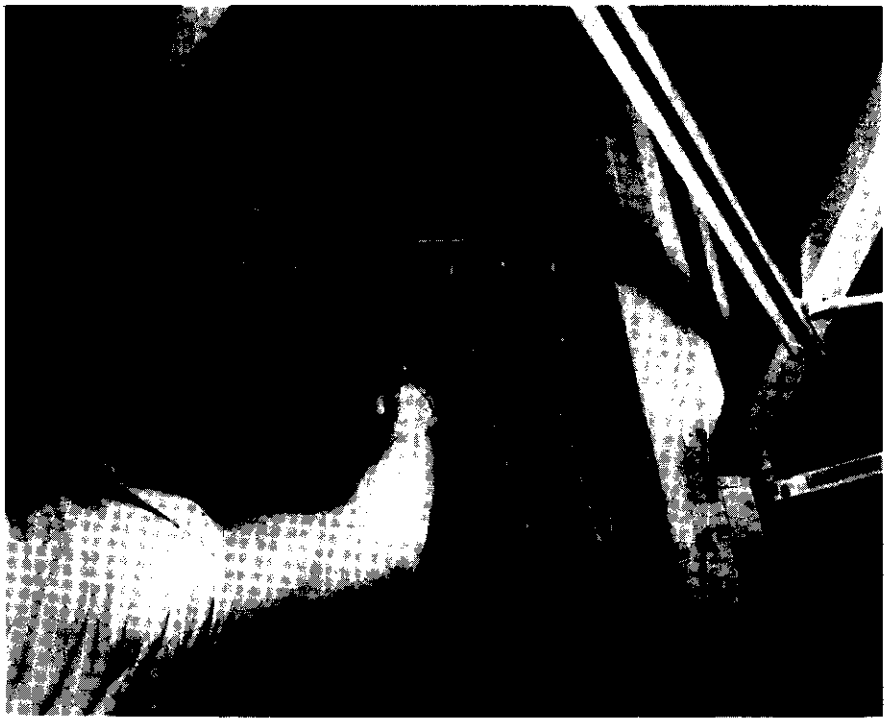

Figure 18. Strings Suspended in the Flow Showing the Direction of Flow with Rainfall.

Figure 19. Dunes on the Bottom of the Flume at Low Velocity without Rainfall.

Figure 20. Dunes on the Bottom of the Flume at Low Velocity with High Rainfall.

rainfall. These samples were depth integrated by manually moving an L-shaped siphon tube from the floor of the flume to the water surface to collect samples. In two replications of 12 samples, the sample means were significantly less at the sides of the flume than at the center at the five per cent level (Table 3).

Measurements indicated that there was no variation in suspended sediment concentration across the flume when rainfall was not imposed on the flow. However, when rainfall was added, differences in suspended sediment concentration existed between the center of the flume and near the sides, with a reduction occurring near the sides. The velocity distribution across the flow indicated that the velocity near the sides of the flume increased and the velocity near the center decreased as a result of rainfall (Tables 8-13, Appendix). Figure 21a shows typical velocity distribution in the flume for tests without rainfall and indicates a maximum velocity at the center. Figure 21b shows the velocity distribution in the flume when rainfall is added and indicates a small increase in velocity near the flume sides. Figure 21c shows the rainfall distribution across the flume.

The nonuniform application of rainfall across the flume may have caused the sediment to have been swept away from the flume bed near the sides during tests with rainfall (Figure 20). This would be expected because the rainfall changed the tractive force distribution across the flume bottom with the zone of maximum tractive force being shifted

Table 3. Suspended Sediment Load Comparisons for the Center and Sides of the Flume

Time (min.)	Left Side		Center		Right Side	
	Test a	Test b	Test a	Test b	Test a	Test b
			Without Rainfall			
00	30	25	29	31	28	29
02	31	31	30	29	31	29
04	30	28	29	29	31	30
06	32	28	29	30	31	27
08	21	28	25	29	27	30
10	30	30	29	27	30	30
12	23	28	29	26	30	27
14	22	31	28	29	29	30
16	30	28	29	30	29	30
18	26	25	29	30	24	30
20	27	28	28	30	26	31
22	30	25	29	32	27	30
Avg.*	28	28	28	29	29	29
			With Rainfall			
30	27	28	25	28	26	22
32	27	26	30	28	28	26
34	25	28	30	30	26	27
36	22	28	31	30	26	27
38	29	28	30	30	30	26
40	22	24	30	32	27	28
42	24	26	29	32	30	26
44	25	26	30	28	27	27
46	24	23	29	28	27	27
48	27	27	29	29	25	24
50	27	28	30	23	30	26
52	28	23	29	26	23	25
Avg.*	26	26	29	29	27	26

Flow conditions:
Velocity - 1.38 ft/sec
Rainfall - 8 psi
Discharge - 1.21 cfs
Temperature - 78°F

Table 3 (cont'd)

Depth integrated samples were taken from the center of the flume and 0.3 feet from each side. The values are the colorimeter readings.

*The student's t-Test was used to compare the means for each replication with and without rainfall. A significant difference at the 5.0 per cent level was found between each side and the center of the flume.

toward the sides of the flume.

It should be noted that with rain, the tendency for the sediment to be deposited from suspension was increased slightly in the center of the flume where rain was most intense. This slight increase could be verified by observing an increase in the size of the dunes along the central portion of the flume bed. The opposite effect of the sediment being swept away from the sides of the flume bed when rain existed was clearly evident (Figure 20).

Two possible explanations for these observed effects are suggested. First, the rainfall decreased the velocity of flow near the surface. This effect was more noticeable near the center of the flume where rainfall was most intense. Since tractive force is related to the velocity gradient, the tractive force was reduced more near the center of the flume than at the edges where it may have increased slightly. However, secondary circulation in the flow, which was increased by rainfall, complicated the flow pattern and may have been the primary reason for the observed results. The increase in surface velocity near the sides of the flume is probably explained by secondary currents moving the zone of maximum velocity away from the center of the flume. This secondary circulation was quite easily observed when rainfall existed (Figure 18).

Instrumentation Error

Errors in the system may be associated with both the flume and its instrumentation. According to Bazin (2), flow in a rectangular channel may be analyzed as being two-dimensional when the bottom width is greater than five times the depth. In the flume used, the construction may have been a source of error. Where the bottom and the sides sections of plywood were joined, cross currents were observed as small standing waves.

Instrumentation error for velocity was calculated as ± 0.15 feet per second, or approximately ± 10 per cent for the velocities studied. This value was obtained by converting the estimated instrument error on the inclined manometer scale to velocity error by using Equation (31). The inclined manometer was read to an accuracy of ± 0.005 inches differential between the manometer fluid and water.

The colorimeter, according to the manufacturer's specifications, is accurate to within one third of one per cent of the full scale reading, which is ± 3 numbers at the maximum reading of 1000 (6). However, for readings of numbers less than 50, as were used in these tests, the error was ± 1 number. This was confirmed by an analysis of 21 homogenious samples of the water and sediment studied, which revealed a maximum variance from the median reading of one whole number on the scale and an average of 0.3 number.

CHAPTER IV

SUMMARY AND RECOMMENDATIONS

Summary

Flume studies were conducted with recirculated flow transporting glass beads to simulate natural sediment in the silt range. The recirculated flow was subjected to simulated rainfall to determine the effects on the flow conditions and the sediment load. Two levels of rainfall and velocity were studied and other variables were held constant. Samples were taken at two-minute intervals for 30 minutes without rainfall and then for the same length of time with rainfall for each of two replications of the conditions.

From this study, the following conclusions may be made:

1. The effects of rainfall on a shallow stream reduce the average velocity slightly, but any resulting changes in sediment transportation are of insufficient magnitudes to be measured by the procedures and equipment utilized.
2. Flow conditions were changed by the addition of a greater amount of rainfall near the center of the flume than at the sides. The reduction in the average velocity which resulted was due to the transfer of momentum from the flowing water to the rainfall. This caused a decrease in the velocity near the center of the flume which resulted in an increase near

the walls. This increase in velocity of flows of lower suspended sediment concentrations was sufficient to remove the sediment from the bottom of the flume. Thus, there was a decrease in the amount of sediment which was placed in the flow due to tractive forces.

3. No change in the variance of concentrations resulted from the addition of rainfall. This indicates that the mixing length and shear velocity were not affected in a manner which would cause a noticeable change in turbulence.

4. Rainfall increases the mass of a flow but imparts no momentum in the direction of flow. Therefore, the velocity must decrease if momentum is to be conserved. This results in a corresponding increase in depth when rainfall is uniform over the channel.

Since natural rainfall is uniform over the width of a natural channel, which is normally shallow near the sides and has its greatest depth near the center, the effects of momentum exchange to the rainfall could produce results opposite to those observed in the flume. That is, since there would be a higher rain-to-flow ratio near the sides of the channel, a slightly greater decrease in flow velocity should occur there in comparison to the central deeper portion of the channel. Hence, a slight flow toward the center of the channel may occur.

This flow would be diluted by the rainfall, which would give it a sediment load of less than the sediment transport capacity of the stream.

Thus, a shallow natural channel might be expected to aggrade near the sides and possibly degrade or remain unchanged at the deeper levels under intense rainfall.

Suggestions for Future Studies

As a result of this study, the following suggestions are made for future studies:

1. Increased sensitivity of velocity measuring equipment is necessary. A velocity probe using a form of strain gage should give increased accuracy. The probe could have a strain gage mounted on a diaphragm situated to detect a pressure differential due to velocity. Compensation for temperature variations could be accomplished by mounting another strain gage near the diaphragm.
2. A continuous flow method of sediment concentration measurements is desirable to permit instantaneous readings. A recording device to facilitate the collection of a large number of readings would be especially desirable.
3. In order that the effects of rainfall on turbulence may be studied, some means of determining instantaneous point velocities in each coordinate direction should be attempted.
4. The dissipation of the kinetic energy of the rainfall is an area which should be studied. Before any positive statements

can be made about the momentum and energy of a flow under rainfall, the disposition of the energy must be determined.

LIST OF REFERENCES

1. Bathke, W. L. Erosion of cohesive soils under shallow channel flow with and without simulated rainfall. M.S. thesis, Texas A&M University, 1963.

2. Bazin, H. Experimental researches on the flow of water in open channels. Academy of Sciences, Paris, vol. 19, 1865.

3. Chow, Ven Te. Handbook of applied hydrology. McGraw-Hill Book Company, Inc., New York, 1964.

4. Chow, Ven Te. Open channel hydraulics. McGraw-Hill Book Company, Inc., New York, 1959.

5. Glass, L. J. The effect of rainfall on the velocity distribution in shallow channel flow. M.S. thesis, Texas A&M University, 1965.

6. Laboratory apparatus and chemicals. Catalog No. 40, W. H. Curtin and Company, Houston, Texas, 1959.

7. Lane, E. W. and Kalinske, A. A. Engineering calculations of suspended sediment. American Geophysical Union, Transactions, 22:603-607, part 3, 1941.

8. Leliavsky, Serge. An introduction to fluvial hydraulics. Constable and Company, Ltd., London, 1959.

9. Li, Jerome C. R. Statistical inference I. Edwards Brothers, Inc., Ann Arbor, Michigan, 1964.

10. Meyer, L. D. and McCune, D. L. Development of a rainfall simulator for runoff plots. Agricultural Engineering, 39:644-648, October, 1958.

11. O'Brien, M. P. Review of the theory of turbulent flow in relation to sediment transportation. American Geophysical Union, Transactions, 14:487. 1933.

12. Rouse, H. Elementary mechanics of fluids. John Wiley and Sons, Inc., New York, 1946.

13. Rouse, H. Engineering hydraulics. John Wiley and Sons, Inc., New York, 1950.

14. Smerdon, E. T. Effect of rainfall on critical tractive forces in channels with shallow flow. American Society of Agricultural Engineering, Transactions, 7:287-290, 1964.

15. Subcommittees on Sedimentation—Interagency Committee on Water Resources. A study of methods used in measurement and analysis of sediment loads in streams. Report #114, Supt. of Doc., USGPO, Washington, D. C., 1963.

16. Trask, P. D. (ed.) Applied sedimentation, John Wiley and Sons, Inc., New York, 1950.

17. Twenhofel, W. H. Principles of sedimentation. McGraw-Hill Book Company, Inc., New York, 1950.

18. West, Wallace. Conserving our waters. Survey by The Committee on Public Affairs of the American Petroleum Institute, 1271 Avenue of the Americas, New York.

19. Wilson, E. Bright, Jr. An introduction to scientific research. McGraw-Hill Book Company, Inc., New York, 1952.

APPENDIX

LIST OF SYMBOLS

Symbol	Description	Dimensions
A	area	L^2
a	Cartesian coordinate reference distance	L
D	diameter of particle	L
d	depth of flow	L
F	force	F
G	mass rate of transfer in the vertical plane	$FL^{-1}T$
g	acceleration of gravity	LT^{-2}
K	proportionality constant	
k	von Karman's constant	
L	length	L
l	mixing length or eddy size	L
n	Manning's roughness coefficient	
Q	discharge	L^3T^{-1}
q	discharge per unit width of flow	L^2T^{-1}
R_e	Reynolds number	
R	hydraulic radius	L
r	radius	L
S_e	slope of the energy gradient	
S_o	slope of the channel	
s	sediment concentration	

t	w/V^*	
$\bar{u}$	average vertical velocity	LT^{-1}
V	horizontal velocity	LT^{-1}
$\bar{V}$	average horizontal velocity	LT^{-1}
V_*	shear velocity, $\sqrt{\frac{\tau_o}{\rho}}$ or $\sqrt{gdS_e}$	LT^{-1}
W	weight	$FL^{-1}T^2$
w	fall velocity	LT^{-1}
y	Cartesian coordinate distance from channel bottom	L
β	constant	
γ	specific weight	FL^{-3}
ϵ_m	kinematic eddy viscosity	L^2T^{-1}
ϵ_s	sediment transfer coefficient	L^2T^{-1}
ξ	shape factor	
η	dynamic viscosity	$FL^{-2}T$
θ	angle	
ν	kinematic viscosity	L^2T^{-1}
π	3.14	
ρ	mass density	$FL^{-4}T^2$
τ	intensity of shear	FL^{-2}
τ_o	intensity of shear at channel bottom	FL^{-2}
ϕ	coefficient of friction	

Table 4. Sediment Data for Conditions of Low Velocity and High Rainfall (Tests 1 and 2)

Without Rainfall			With Rainfall		
		y = 0.32 foot			
Time (min)	Reading Test 1	Test 2	Time	Reading Test 1	Test 2
00	21	20	36	15	21
02	18	21	38	12	18
04	18	19	40	13	18
06	21	14	42	10	16
08	19	20	44	15	15
10	13	18	46	11	15
12	20	14	48	13	15
14	20	21	50	15	13
16	16	17	52	17	13
18	19	18	54	15	11
20	20	18	56	18	11
22	18	14	58	13	14
24	18	21	60	19	15
26	15	21	62	16	13
28	13	15	64	15	12
30	14	15	66	14	12
		y = 0.22 foot			
00	26	25	36	22	17
02	20	25	38	18	17
04	26	20	40	16	17
06	19	15	42	17	23
08	17	12	44	21	17
10	19	17	46	18	21
12	20	13	48	17	16
14	13	19	50	17	18
16	17	17	52	11	13
18	17	17	54	14	18
20	18	17	56	18	12
22	17	15	58	11	16
24	20	16	60	13	16
26	18	12	62	23	18
28	22	16	64	22	14
30	16	18	66	23	20

Table 4. (Cont'd)

Without Rainfall			With Rainfall		
		y = 0.12 foot			
Time (min)	Reading Test 1	Test 2	Time	Reading Test 1	Test 2
00	20	16	36	14	16
02	25	25	38	20	24
04	19	16	40	21	24
06	16	18	42	18	18
08	17	17	44	14	16
10	22	18	46	14	14
12	16	15	48	18	16
14	17	13	50	17	19
16	21	21	52	10	22
18	18	20	54	13	22
20	19	21	56	14	24
22	21	23	58	14	24
24	23	20	60	18	15
26	16	18	62	19	17
28	20	25	64	15	21
30	21	18	66	20	19
		y = 0.02 foot			
00	22	23	36	21	21
02	22	30	38	20	20
04	22	26	40	15	23
06	18	23	42	15	23
08	20	16	44	15	17
10	21	21	46	19	15
12	19	13	48	18	17
14	15	14	50	19	19
16	17	18	52	19	19
18	19	20	54	15	17
20	19	15	56	16	17
22	18	20	58	17	19
24	18	17	60	17	17
26	17	19	62	17	18
28	14	16	64	15	18
30	20	13	66	18	16

Table 4 (cont'd)

Without Rainfall			With Rainfall		
Total Load					
Time (min)	Reading Test 1	Test 2	Time (min)	Reading Test 1	Test 2
00	22	18	36	20	17
02	21	25	38	13	17
04	19	18	40	16	19
06	18	18	42	16	13
08	17	23	44	13	14
10	16	15	46	15	16
12	20	19	48	12	16
14	16	19	50	12	18
16	14	17	52	15	13
18	12	14	54	10	15
20	18	14	56	12	10
22	17	17	58	15	15
24	19	16	60	16	14
26	19	16	62	12	16
28	22	16	64	16	13
30	22	14	66	17	15

Flow conditions: Velocity - 1.38 ft/sec
Rainfall - 8 lb/in.^{2}
Discharge - 1.21 ft^3/sec
Temperature - 78°F.

Table 5. Sediment Data for Conditions of Low Velocity and Low Rainfall (Tests 3 and 4)

Without Rainfall			With Rainfall		
y = 0.32 foot					
Time (min)	Reading Test 3	Test 4	Time (min)	Reading Test 3	Test 4
00	28	20	36	16	22
02	31	19	38	21	20
04	28	21	40	20	19
06	27	23	42	18	16
08	19	24	44	18	17
10	22	20	46	18	12
12	19	18	48	15	16
14	16	19	50	18	16
16	15	19	52	19	18
18	20	15	54	23	17
20	23	21	56	15	17
22	20	20	58	18	18
24	18	22	60	20	17
26	14	20	62	18	19
28	15	20	64	15	18
30	20	17	66	17	15
y = 0.22 foot					
00	32	26	36	18	22
02	30	25	38	21	17
04	31	21	40	17	15
06	26	23	42	17	19
08	20	24	44	15	19
10	19	22	46	17	17
12	18	21	48	13	17
14	23	19	50	13	17
16	18	20	52	21	15
18	22	19	54	22	13
20	21	21	56	25	10
22	18	22	58	23	15
24	17	16	60	19	14
26	16	20	62	21	12
28	19	19	64	18	11
30	17	15	66	19	10

Table 5. (cont'd)

Without Rainfall			With Rainfall		
y = 0.12 foot					
Time (min)	Reading Test 3	Test 4	Time (min)	Reading Test 3	Test 4
00	35	28	36	22	19
02	34	25	38	18	19
04	32	20	40	25	21
06	23	23	42	21	21
08	20	24	44	22	15
10	23	24	46	25	21
12	18	22	48	20	21
14	23	23	50	22	19
16	20	21	52	22	23
18	21	21	54	26	24
20	15	15	56	23	19
22	25	20	58	25	22
24	20	20	60	17	21
26	13	18	62	23	22
28	19	16	64	21	22
30	16	16	66	24	22
y = 0.02 foot					
00	32	26	36	25	20
02	21	19	38	22	23
04	32	25	40	21	25
06	28	26	42	16	25
08	20	21	44	23	19
10	20	22	46	24	23
12	18	22	48	20	24
14	22	20	50	22	20
16	26	20	52	20	17
18	17	23	54	23	18
20	25	25	56	25	14
22	18	21	58	16	17
24	20	22	60	20	17
26	19	24	62	25	22
28	16	25	64	20	17
30	20	27	66	22	21

Table 5 (cont'd)

Without Rainfall			With Rainfall		
Total Load					
Time (min)	Reading Test 3	Test 4	Time (min)	Reading Test 3	Test 4
00	26	24	36	15	18
02	18	26	38	17	18
04	23	19	40	21	18
06	19	19	42	18	20
08	25	22	44	19	20
10	22	22	46	18	19
12	23	25	48	14	19
14	22	24	50	17	17
16	21	26	52	16	19
18	22	25	54	16	20
20	20	20	56	17	21
22	21	20	58	14	24
24	21	20	60	17	24
26	24	18	62	17	25
28	24	16	64	17	23
30	22	20	66	18	24

Flow conditions: Velocity - 1.38 ft/sec
Rainfall - 5 lb/in.^{2}
Discharge - 1.21 ft^3/sec
Temperature - 78° F.

Table 6. Sediment Data for Conditions of High Velocity and High Rainfall (Tests 5 and 6)

Without Rainfall			With Rainfall		
y = 0.32 foot					
Time (min)	Reading		Time (min)	Reading	
	Test 5	Test 6		Test 5	Test 6
00	15	35	36	22	25
02	21	29	38	17	22
04	19	26	40	22	22
06	22	25	42	22	22
08	25	25	44	20	22
10	25	21	46	16	22
12	25	16	48	18	21
14	26	16	50	19	20
16	25	17	52	22	23
18	25	18	54	17	19
20	18	22	56	19	22
22	17	21	58	22	19
24	27	19	60	17	18
26	19	17	62	20	23
28	17	20	64	20	23
30	15	16	66	16	20
y = 0.22 foot					
00	22	27	36	23	20
02	21	28	38	22	25
04	19	26	40	22	25
06	28	25	42	24	26
08	25	27	44	24	26
10	27	26	46	18	25
12	20	26	48	20	28
14	31	24	50	21	28
16	20	24	52	22	27
18	21	25	54	22	27
20	23	25	56	18	26
22	19	23	58	18	25
24	25	19	60	18	26
26	18	20	62	19	19
28	17	18	64	19	20
30	17	22	66	19	19

Table 6. (cont'd)

Without Rainfall			With Rainfall		
		y = 0.12 foot			
Time (min)	Reading Test 5	Test 6	Time (min)	Reading Test 5	Test 6
00	27	35	36	18	30
02	25	30	38	15	25
04	22	32	40	22	22
06	28	26	42	24	20
08	28	28	44	20	27
10	25	32	46	17	31
12	24	29	48	23	30
14	31	31	50	20	28
16	22	34	52	18	27
18	23	27	54	21	18
20	25	24	56	21	30
22	20	33	58	18	28
24	18	30	60	18	32
26	19	27	62	18	31
28	16	32	64	15	31
30	18	35	66	20	30
		y = 0.02 foot			
00	23	32	36	21	20
02	27	28	38	25	30
04	29	26	40	25	29
06	28	26	42	24	26
08	25	28	44	23	30
10	25	24	46	25	31
12	26	20	48	25	30
14	31	21	50	24	29
16	21	23	52	15	29
18	24	25	54	21	23
20	28	25	56	22	24
22	20	23	58	22	28
24	20	29	60	18	28
26	17	27	62	22	27
28	16	32	64	22	26
30	21	25	66	25	24

Table 6 (cont'd)

Without Rainfall			With Rainfall		
Total Load					
Time (min)	Reading Test 5	Test 6	Time (min)	Reading Test 5	Test 6
00	27	28	36	23	24
02	25	28	38	25	28
04	20	28	40	25	28
06	22	28	42	25	29
08	16	22	44	25	29
10	22	26	46	25	27
12	21	26	48	28	30
14	19	26	50	28	32
16	20	25	52	25	30
18	20	26	54	25	26
20	21	24	56	25	22
22	22	24	58	26	22
24	22	23	60	20	26
26	23	22	62	22	25
28	25	21	64	23	28
30	25	21	66	23	31

Flow conditions: Velocity - 1.55 ft/sec
Rainfall - 8 lb/in.^{2}
Discharge - 1.36 ft^3/sec
Temperature - 78°F.

Table 7. Sediment Data for Conditions of High Velocity and Low Rainfall. (Tests 7 and 8)

Without Rainfall			With Rainfall		
y = 0.32 foot					
Time (min)	Reading		Time (min)	Reading	
	Test 7	Test 8		Test 7	Test 8
00	27	27	36	27	24
02	31	27	38	28	27
04	23	28	40	28	24
06	24	25	42	24	25
08	22	25	44	20	27
10	22	27	46	22	25
12	24	23	48	31	23
14	22	19	50	22	30
16	22	25	52	26	24
18	19	23	54	22	21
20	20	24	56	23	26
22	26	18	58	24	26
24	31	22	60	21	23
26	22	21	62	19	25
28	22	24	64	23	29
30	25	23	66	18	21
y = 0.22 foot					
00	35	25	36	27	20
02	27	32	38	26	26
04	29	29	40	29	26
06	30	23	42	27	26
08	28	30	44	26	27
10	28	31	46	27	26
12	30	25	48	31	27
14	26	25	50	28	31
16	27	26	52	30	26
18	27	25	54	21	28
20	24	25	56	26	31
22	31	25	58	24	29
24	25	26	60	27	30
26	23	25	62	29	33
28	24	25	64	28	27
30	29	25	66	26	27

Table 7 (cont'd)

Without Rainfall			With Rainfall		
		y = 0.12 foot			
Time (min)	Reading Test 7	Test 8	Time (min)	Reading Test 7	Test 8
00	35	32	36	30	31
02	33	29	38	30	27
04	30	27	40	30	29
06	33	33	42	31	30
08	31	25	44	25	30
10	31	29	46	30	30
12	23	28	48	26	30
14	24	28	50	29	29
16	25	24	52	26	30
18	32	26	54	25	30
20	31	23	56	30	30
22	35	30	58	28	30
24	30	25	60	29	30
26	28	23	62	29	32
28	28	27	64	30	26
30	30	29	66	26	25
		y = 0.02 foot			
00	32	23	36	25	35
02	34	23	38	24	36
04	34	24	40	31	30
06	35	36	42	27	30
08	27	22	44	30	32
10	32	20	46	35	30
12	31	18	48	25	32
14	31	20	50	24	30
16	29	25	52	33	28
18	29	28	54	30	28
20	30	28	56	22	26
22	23	26	58	22	26
24	28	21	60	33	26
26	27	28	62	23	28
28	24	24	64	25	23
30	23	30	66	33	24

Table 7. (cont'd)

Without Rainfall			With Rainfall		
Total Load					
Time (min)	Reading		Time (min)	Reading	
	Test 7	Test 8		Test 7	Test 8
00	27	26	36	21	22
02	25	20	38	18	23
04	27	26	40	18	20
06	25	20	42	24	26
08	24	20	42	27	22
10	21	25	46	27	22
12	28	23	48	26	18
14	24	21	50	29	15
16	24	24	52	26	11
18	25	23	54	22	20
20	19	20	56	22	22
22	21	23	58	25	26
24	21	20	60	23	26
26	21	23	62	23	17
28	19	25	64	23	24
30	21	25	66	26	24

Flow conditions: Velocity - 1.55 ft/sec
Rainfall - 8 lb/in.^{2}
Discharge - 1/36 ft^3/sec
Temperature - 78°F.

Table 8. Point Velocity Data for Conditions of Low Velocity and No Rainfall

Width (feet) / Depth (feet)	0.04	0.40	0.80	1.00	1.25	1.50	1.70	2.10
0.32	1.31	1.62	1.64	1.65	1.65	1.65	1.64	1.64
0.30	1.32	1.54	1.67	1.67	1.65	1.65	1.65	1.61
0.25	1.35	1.57	1.67	1.67	1.64	1.64	1.61	1.61
0.20	1.25	1.61	1.62	1.62	1.61	1.59	1.61	1.51
0.15	1.27	1.54	1.52	1.51	1.51	1.51	1.45	1.51
0.10	1.27	1.47	1.47	1.47	1.47	1.47	1.45	1.46
0.05	1.23	1.32	1.38	1.36	1.33	1.33	1.33	1.36
0.02		1.18	1.18	1.18	1.18	1.18	1.16	1.18

Table 9. Point Velocity Data for Conditions of Low Velocity and High Rainfall

Width (feet) / Depth (feet)	0.04	0.40	0.80	1.00	1.25	1.50	1.70	2.10
0.32	1.48	1.61	1.62	1.62	1.59	1.58	1.51	1.52
0.30	1.50	1.62	1.61	1.62	1.61	1.61	1.50	1.52
0.25	1.51	1.62	1.63	1.61	1.61	1.50	1.46	1.52
0.20	1.47	1.61	1.59	1.57	1.52	1.50	1.46	1.54
0.15	1.41	1.50	1.48	1.47	1.46	1.42	1.39	1.45
0.10	1.25	1.47	1.39	1.38	1.35	1.32	1.28	1.32
0.05	1.16	1.23	1.25	1.25	1.23	1.23	1.18	1.25
0.02		1.21	1.16	1.15	1.11	1.13	1.10	1.10

Table 10. Point Velocity Data for Conditions of Low Velocity and Low Rainfall

Width (feet) / Depth (feet)	0.04	0.40	0.80	1.00	1.25	1.50	1.70	2.10
0.32	1.61	1.63	1.61	1.62	1.59	1.54	1.54	1.54
0.30	1.61	1.63	1.62	1.62	1.59	1.57	1.51	1.48
0.25	1.61	1.61	1.62	1.55	1.54	1.50	1.47	1.50
0.20	1.46	1.48	1.55	1.55	1.52	1.51	1.47	1.50
0.15	1.50	1.54	1.51	1.51	1.50	1.42	1.36	1.38
0.10	1.36	1.50	1.50	1.44	1.44	1.38	1.33	1.35
0.05	1.10	1.27	1.28	1.28	1.25	1.21	1.13	1.27
0.02	1.13	1.23	1.20	1.20	1.15	1.13	1.10	1.06

Table 11. Point Velocity Data for Conditions of High Velocity and No Rainfall

Width (feet) / Depth (feet)	0.04	0.40	0.80	1.00	1.25	1.50	1.70	2.10
0.32	1.44	1.72	1.77	1.80	1.83	1.82	1.81	1.80
0.30	1.44	1.67	1.69	1.75	1.80	1.81	1.81	1.80
0.25	1.44	1.69	1.69	1.71	1.74	1.74	1.72	1.72
0.20	1.44	1.61	1.63	1.62	1.67	1.69	1.63	1.68
0.15	1.44	1.57	1.55	1.51	1.54	1.54	1.51	1.58
0.10	1.44	1.52	1.50	1.50	1.50	1.47	1.48	1.55
0.05	1.36	1.42	1.44	1.44	1.38	1.36	1.41	1.36
0.02	1.13	1.21	1.25	1.25	1.27	1.27	1.21	1.25

Table 12. Point Velocity Data for Conditions of High Velocity and High Rainfall

Width (feet) / Depth (feet)	0.04	0.40	0.80	1.00	1.25	1.50	1.70	2.10
0.32	1.39	1.69	1.67	1.67	1.63	1.63	1.62	1.63
0.30	1.45	1.74	1.71	1.68	1.64	1.62	1.57	1.68
0.25	1.52	1.77	1.68	1.64	1.64	1.62	1.57	1.63
0.20	1.46	1.76	1.57	1.54	1.52	1.51	1.48	1.58
0.15	1.38	1.72	1.55	1.48	1.47	1.45	1.39	1.63
0.10	1.25	1.61	1.30	1.28	1.38	1.38	1.30	1.61
0.05	1.25	1.36	1.27	1.23	1.23	1.23	1.23	1.30
0.02	1.20	1.30	1.16	1.16	1.16	1.15	1.11	1.25

Table 13. Point Velocity Data for Conditions of High Velocity and Low Rainfall

Width (feet) / Depth (feet)	0.04	0.40	0.80	1.00	1.25	1.50	1.70	2.10
0.32	1.51	1.63	1.63	1.64	1.63	1.64	1.64	1.67
0.30	1.47	1.64	1.63	1.63	1.63	1.64	1.63	1.64
0.25	1.42	1.63	1.63	1.62	1.63	1.62	1.62	1.63
0.20	1.50	1.59	1.57	1.57	1.55	1.51	1.50	1.57
0.15	1.45	1.50	1.47	1.47	1.47	1.48	1.42	1.51
0.10	1.23	1.44	1.36	1.36	1.36	1.36	1.35	1.38
0.05	1.10	1.25	1.23	1.21	1.25	1.23	1.20	1.27
0.02	1.11	1.23	1.16	1.16	1.20	1.13	1.11	1.21

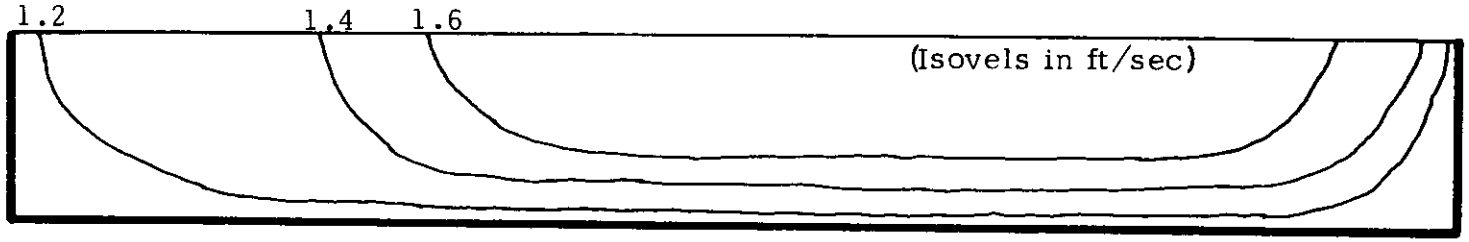

a. Velocity distribution with low velocity and no rainfall

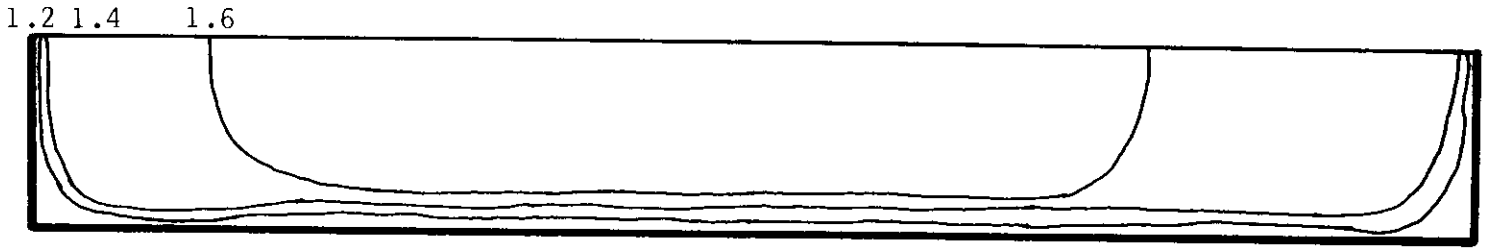

b. Velocity distribution with low velocity and high rainfall

c. Rainfall intensity distribution across the flume with high rainfall

Figure 21. Typical Velocity and Rainfall Distributions in the Flume (Scale: 3 inches = 1 foot)